

# Australian Journal of Earth Sciences

An International Geoscience Journal of the Geological Society of Australia

ISSN: 0812-0099 (Print) 1440-0952 (Online) Journal homepage: <http://www.tandfonline.com/loi/taje20>

## Evidence for hybridisation in the Tynong Province granitoids, Lachlan Fold Belt, eastern Australia

K. R. Regmi, R. F. Weinberg, I. A. Nicholls, R. Maas & M. Raveggi

To cite this article: K. R. Regmi, R. F. Weinberg, I. A. Nicholls, R. Maas & M. Raveggi (2016): Evidence for hybridisation in the Tynong Province granitoids, Lachlan Fold Belt, eastern Australia, Australian Journal of Earth Sciences, DOI: [10.1080/08120099.2016.1180321](https://doi.org/10.1080/08120099.2016.1180321)

To link to this article: <http://dx.doi.org/10.1080/08120099.2016.1180321>

 View supplementary material 

 Published online: 07 Jul 2016.

 Submit your article to this journal 

 Article views: 18

 View related articles 

 View Crossmark data 

## Evidence for hybridisation in the Tynong Province granitoids, Lachlan Fold Belt, eastern Australia

K. R. Regmi<sup>a,b</sup>, R. F. Weinberg<sup>a</sup>, I. A. Nicholls<sup>a</sup>, R. Maas<sup>c</sup> and M. Raveggi<sup>a</sup>

<sup>a</sup>School of Earth, Atmosphere and Environment, Monash University, Clayton, VIC 3800, Australia; <sup>b</sup>Department of Geology, Faculty of Science, University of Namibia, Windhoek, Namibia; <sup>c</sup>School of Earth Sciences, University of Melbourne, VIC 3010, Australia

### ABSTRACT

The role of mafic–felsic magma mixing in the formation of granites is controversial. Field evidence in many granite plutons undoubtedly implies interaction of mafic (basaltic–intermediate) magma with (usually) much more abundant granitic magma, but the extent of such mixing and its effect on overall chemical features of the host intrusion are unclear. Late Devonian I-type granitoids of the Tynong Province in the western Lachlan Fold Belt, southeast Australia, show typical evidence for magma mingling and mixing, such as small dioritic stocks, hybrid zones with local host granite and ubiquitous microgranitoid enclaves. The latter commonly have irregular boundaries and show textural features characteristic of hybridisation, e.g. xenocrysts of granitic quartz and K-feldspars, rapakivi and antirapakivi textures, quartz and feldspar ocelli, and acicular apatite. Linear (well defined to diffuse) compositional trends for granites, hybrid zones and enclaves have been attributed to magma mixing but could also be explained by other mechanisms. Magmatic zircons of the Tynong and Toorongo granodiorites yield U–Pb zircon ages consistent with the known *ca* 370 Ma age of the province and preserve relatively unevolved  $\epsilon_{\text{Hf}}$  (averages for three samples are +6.9, +4.3 and +3.9). The range in zircon  $\epsilon_{\text{Hf}}$  in two of the three analysed samples (8.8 and 10.1  $\epsilon_{\text{Hf}}$  units) exceeds that expected from a single homogeneous population ( $\sim 4$  units) and suggests considerable Hf isotopic heterogeneity in the melt from which the zircon formed, consistent with syn-intrusion magma mixing. Correlated whole-rock Sr–Nd isotope data for the Tynong Province granitoids show a considerable range (0.7049–0.7074,  $\epsilon_{\text{Nd}}$  +1.2 to –4.7), which may map the hybridisation between a mafic magma and possibly multiple crustal magmas. Major-element variations for host granite, hybrid zones and enclaves in the large Tynong granodiorite show correlations with major-element compositions of the type expected from mixing of contrasting mafic and felsic magmas. However, chemical–isotopic correlations are poorly developed for the province as a whole, especially for  $^{87}\text{Sr}/^{86}\text{Sr}$ . In a magma mixing model, such complexities could be explained in terms of a dynamic mixing/mingling environment, with multiple mixing events and subsequent interactions between hybrids and superimposed fractional crystallisation. The results indicate that features plausibly attributed to mafic–felsic magma mixing exist at all scales within this granite province and suggest a major role for magma mixing/mingling in the formation of I-type granites.

### ARTICLE HISTORY

Received 15 September 2015  
Accepted 12 April 2016

### KEYWORDS:

magma mixing;  
hybridisation; Hf isotopes;  
zircon; Tynong Province;  
Lachlan Orogen

### Introduction

Magma mixing between mantle-derived mafic magmas and crust-derived felsic magmas is one of the key processes underlying magma differentiation, leading to hybrid isotopic signatures, as well as mingling structures preserved owing to partial mixing, and documented in both plutonic and volcanic environments (Bonin, 2004; Collins, 1996; Eberz, Nicholls, Maas, McCulloch, & Whiteford, 1990; Elburg & Nicholls, 1995; Gray & Kemp, 2009; Keay, Collins, & McCulloch, 1997; Kemp & Hawkesworth, 2003; Perugini, De Campos, Ertel-Ingrisch, & Dingwell, 2012; Poli, Tommasini, & Halliday, 1996; Vernon, Etheridge, & Wall, 1988; Waight, Dean, Maas, & Nicholls, 2000; Wall, Clemens, & Clarke, 1987; Wiebe, 1993, 1994). A number of processes have been suggested to explain I-type granitoid

suites of the Lachlan Fold Belt, eastern Australia, from the classic restite unmixing model (e.g. White & Chappell, 1977) to fractionation (Soesoo, 2000; Wyborn, Chappell, & James, 2001). Geochemical trends, isotopic compositions and field relationships have led many authors to argue that mixing between two end-member magmas underlies the evolution of many I-type granitoid suites in the Lachlan Fold Belt (Collins, 1998; Gray, 1984; Gray & Kemp, 2009; Keay et al., 1997) challenging previous interpretations that the suites were a result of restite unmixing (White & Chappell, 1977). Adding further complexity, Keay et al. (1997) and Collins (1998) suggested that the I-type granitoids of the Lachlan Fold Belt may have been a mixture of components from three sources: Cambrian mafic oceanic or arc metavolcanic rocks of the

lower to mid-crust, Ordovician marine metasedimentary rocks and mantle-derived magma.

This paper investigates magma hybridisation by linking field and petrographic evidence with the results of whole-rock major and trace-element geochemistry, Sm–Nd and Rb–Sr isotopic studies and Hf isotopic data for zircons from granitoids of the Tynong Province, Lachlan Fold Belt. In addition, new U–Pb zircon dating of the granitoids is presented. These data are used to explore the origin of the granitoids and constrain granite petrogenesis.

Chappell (1996) questioned the role of large-scale magma mixing or mingling as a significant process in the genesis of granitoids. However, he accepted that small amounts of mingling took place in some plutons. Likewise, Clemens and co-authors have proposed that the Peritectic Assemblage Entrainment (PAE) model could explain geochemical variation in some of these plutons (Clemens & Bezuidenhout, 2014) as well as elsewhere. Clemens and Stevens (2012) summarise PAE in the following way:

... once a partial melt has formed in a crustal protolith it may segregate from its complementary solid residue carrying small crystals of the peritectic phase assemblage formed in the melting reaction, and that the ratios of individual peritectic minerals in the entrained assemblage remain fixed in the ratio decreed by the stoichiometry of the melting reaction. For those elements with low solubilities in granitic melts, PAE (in varying degrees), accompanied by co-entrainment of accessory minerals, is responsible for most of the primary elemental variation in granitic magmas.

We will return to this theme in the discussion.

Mafic–intermediate microgranitoid enclaves (MME), common in intermediate to felsic granitoids, preserve information about the chemical and physical evolutionary history of the parental magmas. Chappell and coworkers (Chappell, White, & Wyborn, 1987; Chappell & Wyborn, 2012; White & Chappell, 1977) interpreted MMEs and gneissic enclaves in granitoids of the Lachlan Fold Belt as representing fragments of source residue re-equilibrated with magma. Clemens and Bezuidenhout (2014) interpreted the two groups of fine-grained enclaves they found in the Lysterfield pluton (one of the bodies studied here) as one group of fragments derived from an early intruded and chilled sill recycled into later magma batches, and another group resulting from hybridisation between mantle and crustal magmas. The latter is in line with the interpretation given by many other authors (Elburg, 1996; Elburg & Nicholls, 1995; Maas, Nicholls, & Legg, 1997; Vernon, 2007; Vernon et al., 1988) who found that some MMEs preserve features best explained by mechanical interaction and rapid cooling of mafic magma globules in felsic magmas. Particularly telling features of this process are the presence of K-feldspar and quartz xenocrysts from the host granite within the MME or straddling their contacts with the felsic host, evidence for mineral disequilibrium such as mantled feldspars, or evidence for rapid cooling of the MME, such as highly acicular apatite crystals (Clemens, Regmi, Nicholls, Weinberg, & Maas, 2016).

Zircons record the isotopic variation of the magma in which they grow and therefore can preserve a record of magma mixing occurring during their growth. Kemp et al. (2007) studied Hf and O isotopes in zircons from the Jindabyne, Why Worry and Cobargo suites of the Lachlan Fold Belt and concluded that they originated by mixing between mantle and crustal magmas. A number of other studies using Lu–Hf isotopes in zircon reached similar conclusions (Belousova, Griffin, & O'Reilly, 2006; Griffin et al., 2002; Hawkesworth & Kemp, 2006; Kemp, Wormald, Whitehouse, & Price, 2005; Kurhila, Anderson, & Ramo, 2010; Yang et al., 2007; Zheng et al., 2007). However, other workers (e.g. Villaros, Buick, & Stevens, 2012), interpreted the heterogeneity in the  $\epsilon_{\text{Hf}}$  values of zircons in granites as reflecting heterogeneity of magma sources.

This paper starts by briefly introducing the regional geology of the Tynong Province, followed by the main observations and results dealing with field relationships, major- and trace-element geochemistry and isotopic studies. Results are discussed in terms of their meaning for the origin and evolution of the granitoids, from which we conclude that the observed variety of rock compositions results from a combination of magma mixing and fractionation.

## Regional geology

The Tynong Batholith, the largest of a group of Late Devonian granitic complexes (Gray & Kemp, 2009) east of Melbourne, includes at least five plutons (Lysterfield, Tynong, Toorongo, Tanjil Bren and Baw Baw plutons; Figure 1), which are exposed in the high country between the Melbourne metropolitan area in the west and the Thomson Reservoir in the east. The plutons lie within the Melbourne (tectonic) Zone (Rossiter, 2003; VandenBerg et al., 2000) and were intruded into strongly folded Lower Ordovician to Lower Devonian turbidite sequences. The Toorongo, Tanjil Bren and Baw Baw plutons, in particular, have produced an unusually broad (2–10 km wide) high temperature contact aureole, including a spectacular zone of partial melting and deformation developed within the quartz-rich metasedimentary country rocks, recording their thermal evolution during and after intrusion of very hot granitic magmas.

The Mornington Peninsula granitoids (Mt Eliza, Mt Martha and Dromana plutons), southwest of the Lysterfield pluton (not shown in Figure 1), also lie within the Melbourne Zone and form part of the Tynong Province, although they are not considered to belong to the Tynong Batholith (Rossiter, 2003). These are the most isotopically primitive granitoids of the Tynong Province (Rossiter, 2003) and are used for comparison.

The Tynong Province occupies the southern portion of the Melbourne Zone and includes only I-type granites. By contrast, the northern part of the Melbourne Zone (the Strathbogie Province of Rossiter, 2003) is dominated by S-type granites and major ignimbrite-filled calderas, the largest

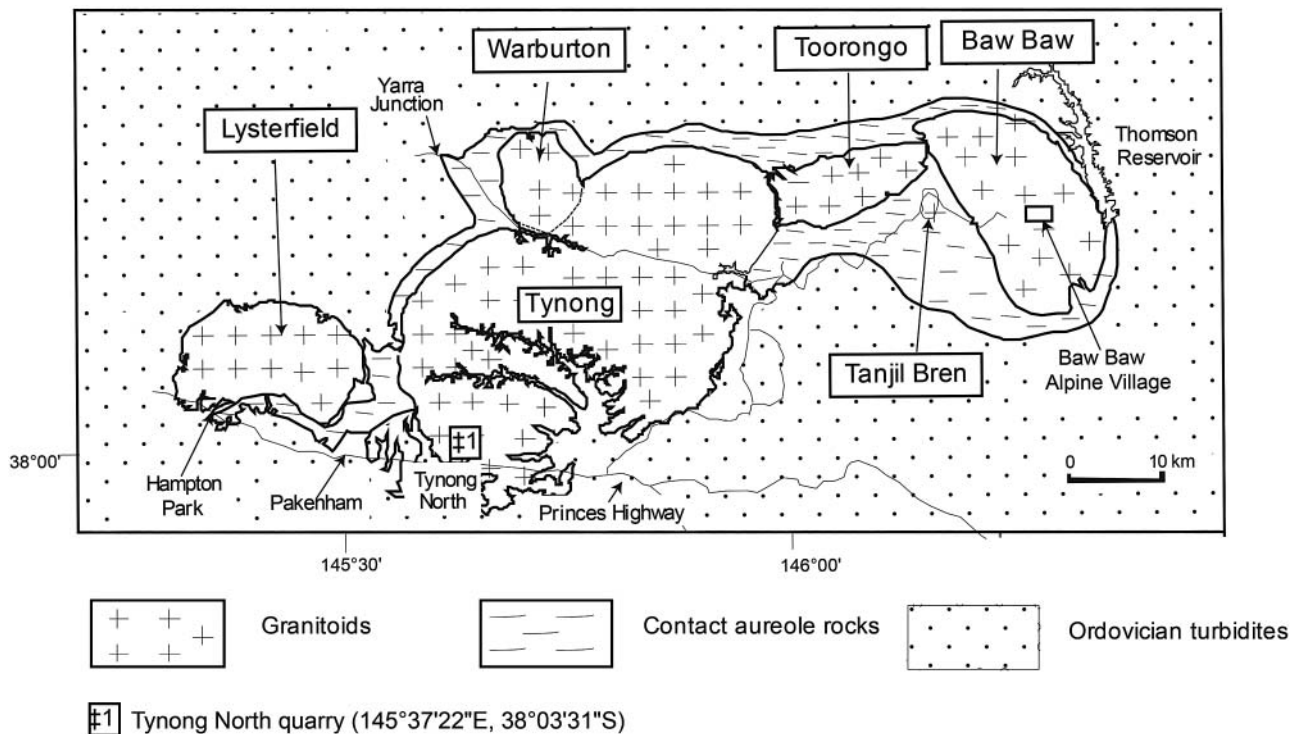


Figure 1. Simplified geological map of Victoria and the study area (modified after Vandenberg et al., 2000).

intrusive complex being the garnet and cordierite-bearing Strathbogie Batholith.

Seismic reflection studies along traverses in central Victoria have allowed detailed interpretation of crustal architecture to Moho depths of  $\sim 35$  km (Cayley et al., 2011; Willman et al., 2010). A prominent feature is the contrast in seismic response of the shallower and deeper parts of the Melbourne Zone. The shallower part (to depths of 10–15 km) is interpreted as consisting of a tightly folded almost continuous sequence of Ordovician to Lower Devonian deep to shallow marine sediments with a lower boundary that shallows towards the south. The basement is interpreted as consisting of at least three layers, the shallowest believed to be Cambrian calc-alkaline volcanic rocks of types exposed in erosion windows along the Governor Fault, the eastern boundary of the Melbourne Zone. The second and third layers are believed to be Proterozoic crust of unspecified type. These three layers are inferred to be components of a lithospheric block—the Selwyn Block—which extends northward from the Proterozoic parts of western Tasmania beneath Bass Strait and at least as far as central Victoria (Cayley, Taylor, Vandenberg, & Moore, 2002; Vandenberg et al., 2000). A prominent feature of most granites of the Melbourne Zone is significant enrichment in Ba, at levels of  $\sim 800$ – $1500$  ppm (Rossiter, 2003; Rossiter & Gray, 2008) that are thought to reflect input from magma sources within metasedimentary rocks forming part of the Selwyn Block.

Clemens and Bezuidenhout (2014) investigated the geochemical evolution of the Lysterfield pluton, and more recently Clemens et al. (2016) have described the Tynong

pluton. These authors minimise the role of magma mixing and fractionation in the origin of components of both these plutons and have defined several groups of related magmatic rocks that they suggest are a result of distinct, initially heterogeneous magmas, aggregated in the pluton. They argued that linear trends defined by some individual groups could be a result of PAE, with a minor role reserved for other processes. They further suggested that the relatively unevolved isotopic signature of the Tynong pluton ( $^{87}\text{Sr}/^{86}\text{Sr}_t \sim 0.705$  to  $0.706$  and  $\epsilon\text{Nd}_{(i)} \sim -0.4$  to  $0.6$ ) could reflect not so much of an addition of juvenile mafic–intermediate magma, but rather the remelting of an equivalent crustal source that had only a short residence time.

### Field relationships and petrography

The Tynong Province granitoids are typically hornblende–biotite granodiorites with large subhedral K-feldspar and plagioclase crystals (commonly as phenocrysts), quartz, biotite and prismatic hornblende (Table 1). Among the Tynong Province granitoids, the Toorongo tonalite–granodiorite is the most mafic, and the Tynong and Tanjil Bren plutons include the most felsic compositions. These granitoids are medium- to coarse-grained and typically have hypidiomorphic granular textures. Some of the rocks of the Tynong Province have experienced minor secondary alteration as evidenced by saussuritisation and sericitisation of plagioclase, chloritisation of biotite and hornblende and locally by the presence of minerals such as clinozoisite/epidote and muscovite. In a few

Table 1. Mineralogical composition of the main granitoid facies in plutons of the Tynong Province.

Pluton	Rock type	Pl	Kfs	Qtz	Hbl	Bt	Ms	Cpx	Zrn	Spn	Aln	Ap	Chl	Ep	Cal	Opq	Pseudomorphs after Opx
Baw Baw	Granodiorites	+++	+++	+++	++	++	–	–	+	+	+	+	+	–	–	+	+
Tanjil Bren	Granites	++	+++	+++	#	++	#	–	+	+	+	+	+	+	#	+	–
Toorongo	Granodiorites	+++	+++	+++	++	++	–	–	+	+	–	+	+	+	–	+	+
Tynong	Granodiorites	+++	+++	+++	++	++	–	–	+	+	–	+	#	+	–	+	–
	Granites	++	+++	+++	#	++	#	–	+	+	+	+	+	+	#	+	–
	Monzogranites	++	++	++	++	++	#	–	+	+	+	+	+	+	#	+	–
	Quartz diorites	+++	+	+	+++	+	–	–	+	+	–	+	–	–	–	+	–
	Enclaves	+++	++	++	++	++	–	+	+	+	–	+	+	–	–	+	+
Lysterfield	Granodiorites	+++	+++	+++	++	++	–	–	+	+	+	+	+	+	–	+	+
	Enclaves	+++	++	++	++	++	–	+	+	+	–	+	+	–	–	+	+

+++ , very abundant; ++ , abundant; + , present; # , trace; – , absent. Abbreviation of mineral names is after Kretz (1983).

samples from the Toorongo pluton Ca-rich clinopyroxene is present (Figure 2), and aggregates of cummingtonite and biotite are interpreted to represent pseudomorphs after orthopyroxene (Figure 3a) or clinopyroxene (Clemens & Bezuidenhout, 2014). The Tynong Province granitoids typically have reddish brown biotite and ilmenite rather than magnetite expected in S-type granitoids. However, the Tynong plutons also contain abundant hornblende and have traditionally been classified as reduced I-type granitoids.

The large Tynong Batholith contains zones of mingling between tens of centimetres to metre-scale bodies of mafic magma and dominant felsic magma. There are two large quarries located in the southern part of the Tynong pluton (Figure 1). Tynong North shows the widest range of diagnostic features of magma mingling and mixing with coeval masses of dioritic rocks, hybrid mixtures of granitic and dioritic rocks and enclaves coexisting with more uniform bodies of dioritic composition (Figure 4). Dioritic rocks also occur as simple and mafic–felsic composite dykes, pods and enclaves. Common enclaves in the granitoids contain large phenocrysts of plagioclase (Figure 3b) and lesser amounts of K-feldspar and quartz and clinopyroxene may also be present (e.g. Baw Baw pluton enclaves; Figure 3d), the latter locally enclosed by hornblende (Figure 3c). Hybrid rocks have quartz and plagioclase surrounded by hornblende forming mantled xenocrysts

(Figure 4d) and such rocks have an increased amount of hornblende relative to other rock types. Very long acicular apatite crystals (aspect ratio >1:5) are present in the quartz diorites (Figure 5) and feldspars commonly have rapakivi and anti-rapakivi textures (Figure 6).

The main differences between these generally similar granitoids are that allanite is absent from granitoids of the Toorongo pluton, and high-T minerals, clinopyroxene and pseudomorphs after orthopyroxene are absent from the Tanjil Bren pluton, whereas the Baw Baw, Lysterfield and Tynong granitoids contain both allanite and pseudomorphs after orthopyroxene (Figure 3a). The Toorongo granodiorite has Ca-clinopyroxene as well as pseudomorphs after orthopyroxene, whereas clinopyroxene is observed only in enclaves in other plutons.

## Methodology

Fragments of samples without abundant alteration were crushed in a bench jaw crusher and further pulverised in a tungsten carbide mill. This material was analysed as follows. X-ray fluorescence analyses were performed at the Advanced Analytical Centre, James Cook University, Townsville. Rare earth and selected trace-element analyses were carried out at Monash University's School of Earth, Atmospheric and Environmental Sciences, following Medlin et al. (2014), using a Thermo Finnigan X series II, quadrupole ICP-MS. Sample solutions were produced from approximately 50 mg of sample powder using high-pressure digestion methods. ICP-MS count rates were externally standardised using curves based on the US Geological Survey standard reference material RGM 1 following Eggins et al. (1997). Drift corrections were based on In and Bi spikes added as internal standards and the repeated analysis of standards interspersed throughout the analytical session. Repeated measurements on standards indicate that precision and accuracy are both around 5% for all elements.

Zircons were separated using standard crushing, magnetic separation and heavy-liquid techniques, and mounted in epoxy. Prior to analytical work, the sectioned and polished grains were imaged on an SEM at the University of Melbourne, to obtain backscattered electron and cathodoluminescence (CL) images that were used to characterise the morphology and the internal structures of the zircons and to choose potential target sites for U–Pb dating and Hf isotopic analyses.

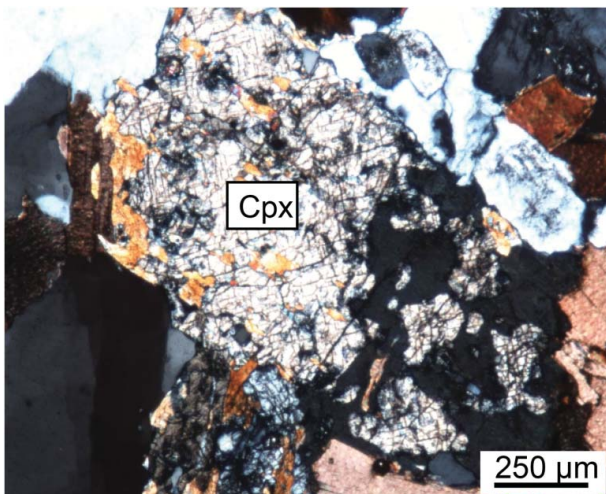


Figure 2. Clinopyroxene (Cpx) in a sample of Toorongo granodiorite (37°48'45"S, 146°02'51"E).

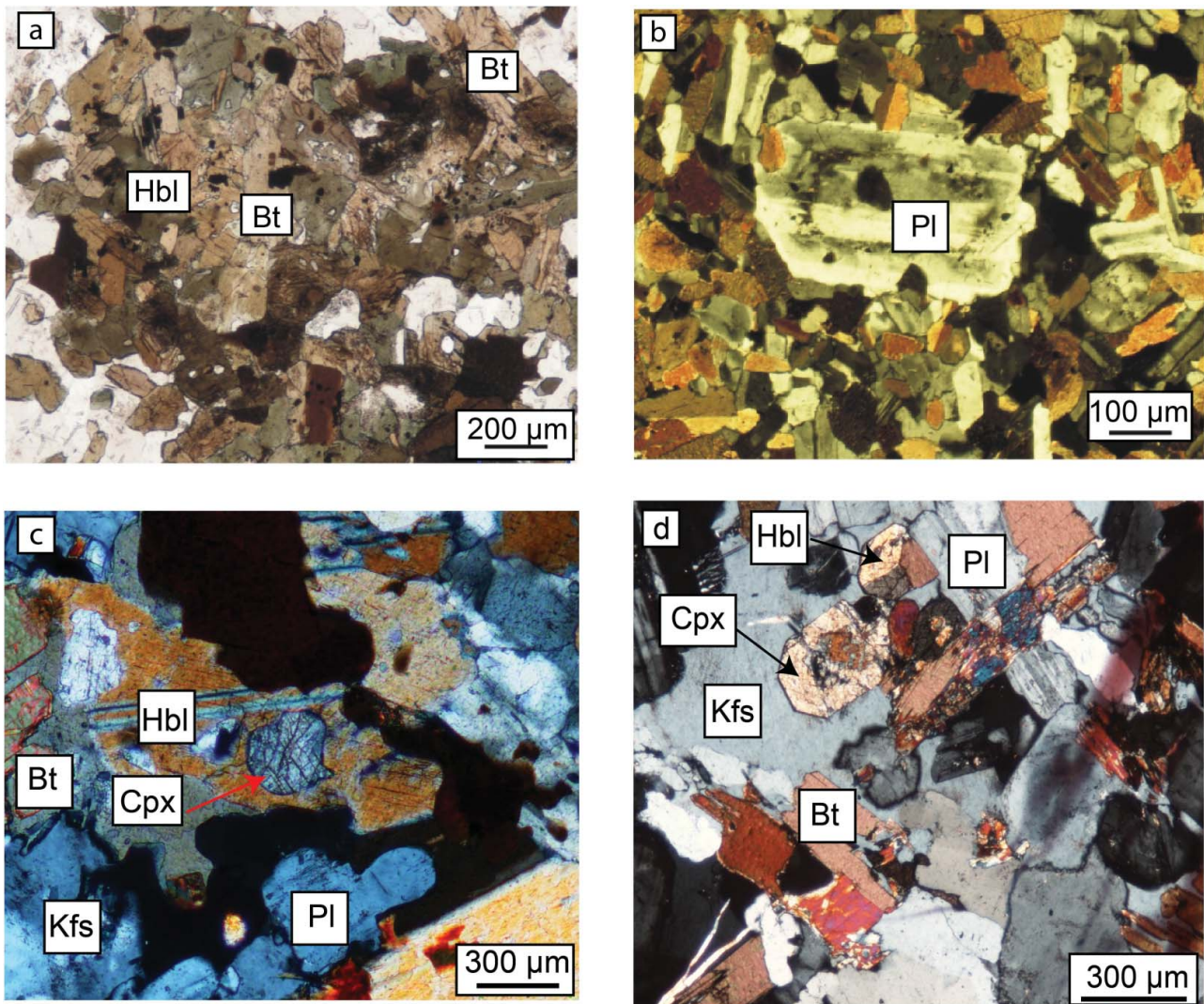


Figure 3. Photomicrographs of representative quartz diorite enclaves from the Tynong Province granitoids: (a) aggregates of hornblende (Hbl) and biotite (Bt) interpreted to represent pseudomorphs after orthopyroxene (Opx) (Lysterfield pluton; 37°55'33"S, 145°21'44"E); (b) phenocrysts of zoned plagioclase (Pl) (Lysterfield pluton; 37°53'02"S, 145°35'47"E); (c) clinopyroxene (Cpx) included by hornblende (Hbl) (Baw Baw pluton; 37°51'01"S, 146°14'26"E), and (d) Clinopyroxene inclusion in poikilitic, interstitial K-feldspar (Baw Baw pluton; 37°51'32"S, 146°15'02"E).

U–Pb zircon dating was carried out by laser ablation ICP–MS at Monash University (Symington et al., 2014), using a Thermo X-series II quadrupole ICP–MS coupled with a New Wave 213 nm, Nd:YAG laser. Zircons were ablated in a mixed He/Ar atmosphere (He/Ar  $\sim$  4/1) with a repetition rate of 5 Hz, 30 μm spot size and approximately 12 mJ cm<sup>-2</sup> of laser energy at the sample. Each analysis consists of a 30 s gas blank followed by 60 s of ablation. The isotopes measured were <sup>90</sup>Zr, <sup>204</sup>Pb, <sup>206</sup>Pb, <sup>207</sup>Pb, <sup>208</sup>Pb, <sup>232</sup>Th and <sup>238</sup>U, with dwell times of 10 ms for <sup>90</sup>Zr and <sup>204</sup>Pb, and 25 ms for the other masses. Instrumental mass bias, drift and down hole fractionation were corrected based on regular analyses of the GJ-1 standard zircon (Jackson, Pearson, Griffin, & Belousova, 2004). The 91500 standard zircon (Wiedenbeck et al., 1995) was used as a secondary standard to assess data quality. Data reduction was done using the GLITTER 4.0 software package (Van Achterbergh, Ryan, Jackson, & Griffin, 2001). External precision for

<sup>238</sup>U/<sup>206</sup>Pb was  $\pm$  4.1% ( $2\sigma$  on 20 analyses) for GJ-1 and  $\pm$  4.7% for 91500; accuracy was  $\sim$   $\pm$  3% ( $2\sigma$  on 20 analyses).

Although <sup>204</sup>Pb was measured, uncorrected interference from <sup>204</sup>Hg and small count rates produced large errors in common-Pb corrections based on <sup>204</sup>Pb. Where required, data were therefore corrected for common Pb using the 207-method (Jackson et al., 2004). The calculations were done with the ISOPLOT v2 software (Ludwig, 2000), using a <sup>207</sup>Pb/<sup>206</sup>Pb common-Pb anchor ratio of 0.8605, equivalent to the ratio at 370 Ma on the Stacey Kramers Pb growth curve (Stacey & Kramers, 1975). Average ages and Tera Wasserburg diagrams were constructed using the ISOPLOT software. The results are presented in Supplementary Papers Tables 1 and 2.

Rb–Sr and Sm–Nd isotopic analyses were carried out at the University of Melbourne (Maas, Kamenetsky, Sobolev, Kamenetsky, & Sobolev, 2005). Powders (50–70 mg) were spiked with <sup>85</sup>Rb–<sup>84</sup>Sr and <sup>149</sup>Sm–<sup>150</sup>Nd tracers and dissolved

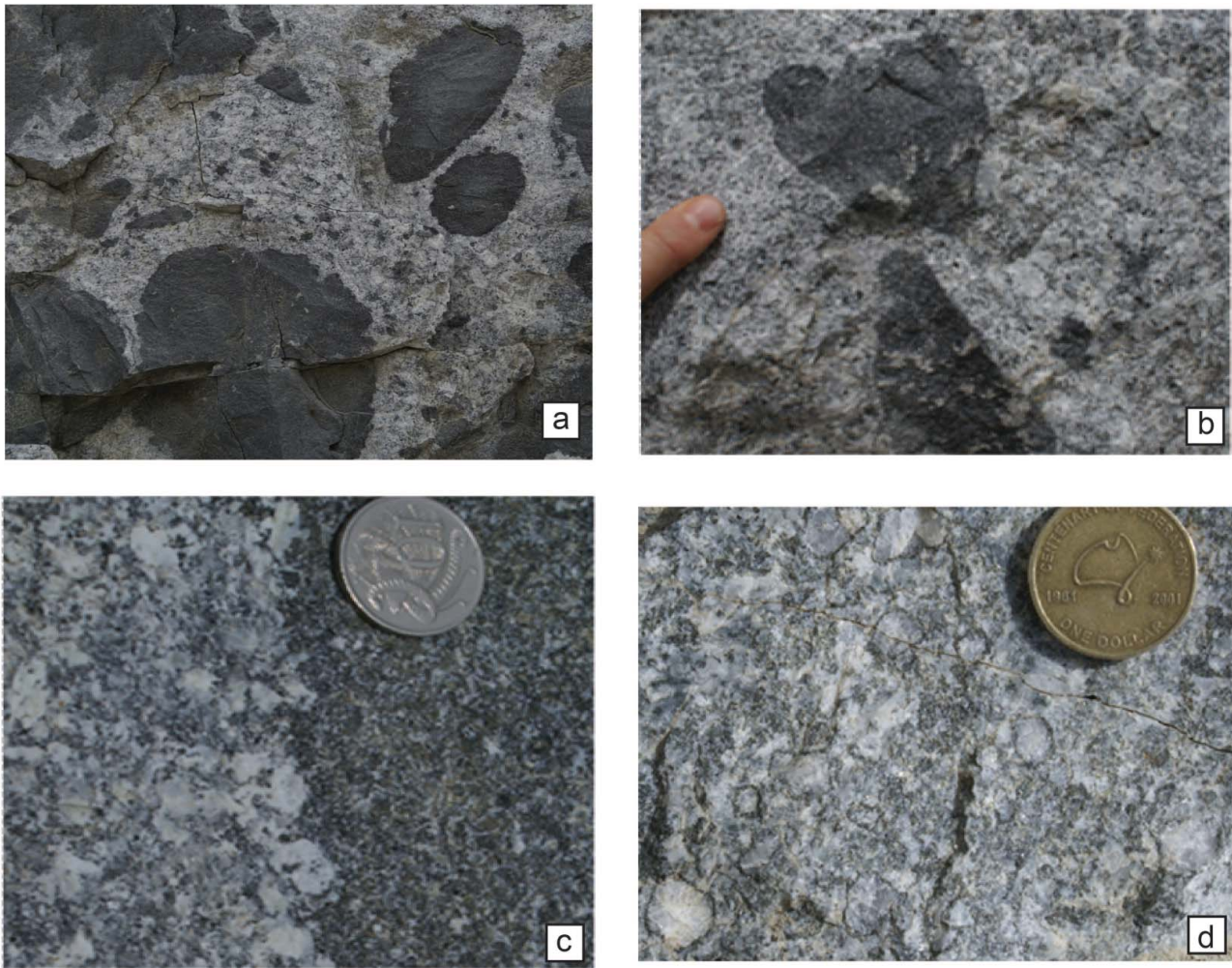


Figure 4. Representative outcrop photographs of the Tynong North Quarry (Figure 1, 38°03'31"S, 145°37'22"E), Tynong pluton. (a, b) Globular MMEs of diorite in granodiorite (view in (a) is approximately 1 m wide); (c) sharp contact between granodiorite and quartz diorite, irregular at grain scale; and (d) granodiorite with quartz (Qtz) and plagioclase (Pl) grains surrounded by hornblende (Hbl) forming ocelli.

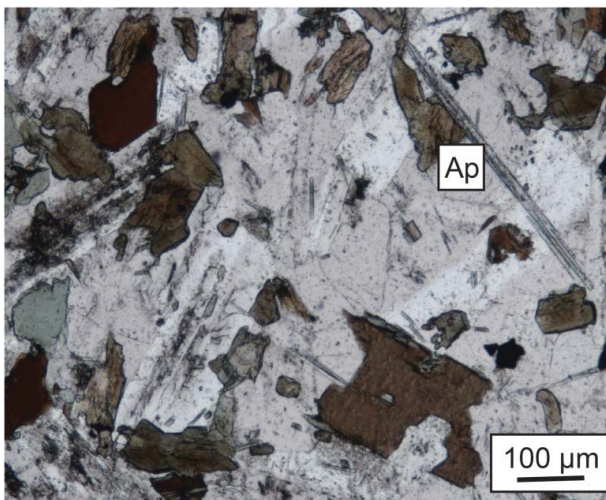


Figure 5. Long apatite (Ap) needle from small intrusive diorite body in Tynong North Quarry.

at high pressure over 3 days. Rb, Sr, Sm and Nd were extracted using conventional cation exchange and Eichrom element specific resins. Isotopic data were obtained on a Nu-Plasma multicollector ICP-MS equipped with an ARIDUS desolvating system. Instrumental mass bias for Sr and Nd was corrected by normalising to  $^{88}\text{Sr}/^{86}\text{Sr} = 8.37521$  and  $^{146}\text{Nd}/^{145}\text{Nd} = 2.0719425$  (equivalent to  $^{146}\text{Nd}/^{144}\text{Nd} = 0.7219$ ; Vance & Thirlwall, 2002), respectively, using the exponential law as part of an on-line iterative spike-stripping/internal normalisation procedure.  $^{87}\text{Sr}/^{86}\text{Sr}$  in SRM987 varied from 0.710269 to 0.710231 ( $n = 4$ ) and from 0.710183 to 0.710222 ( $n = 3$ ) in the relevant analytical sessions, and final  $^{87}\text{Sr}/^{86}\text{Sr}$  ratios are reported relative to SRM987 = 0.710230.  $^{143}\text{Nd}/^{144}\text{Nd}$  in La Jolla Nd varied from 0.511705 to 0.511759 ( $n = 11$ ) and from 0.511664 to 0.511693 ( $n = 11$ ), and final  $^{143}\text{Nd}/^{144}\text{Nd}$  ratios are reported relative to a ratio of 0.511860. Typical in-run precisions (2SD) are  $\pm 0.000020$  (Sr) and  $\pm 0.000010$  (Nd); external precision (reproducibility, 2SD) is  $\pm 0.000040$  (Sr) and  $\pm 0.000020$  (Nd). Rb isotope dilution analyses were made using Zr-doping (Waight, Baker, & Willigers, 2002). External precisions for  $^{87}\text{Rb}/^{86}\text{Sr}$  and  $^{147}\text{Sm}/^{144}\text{Nd}$  obtained by isotope

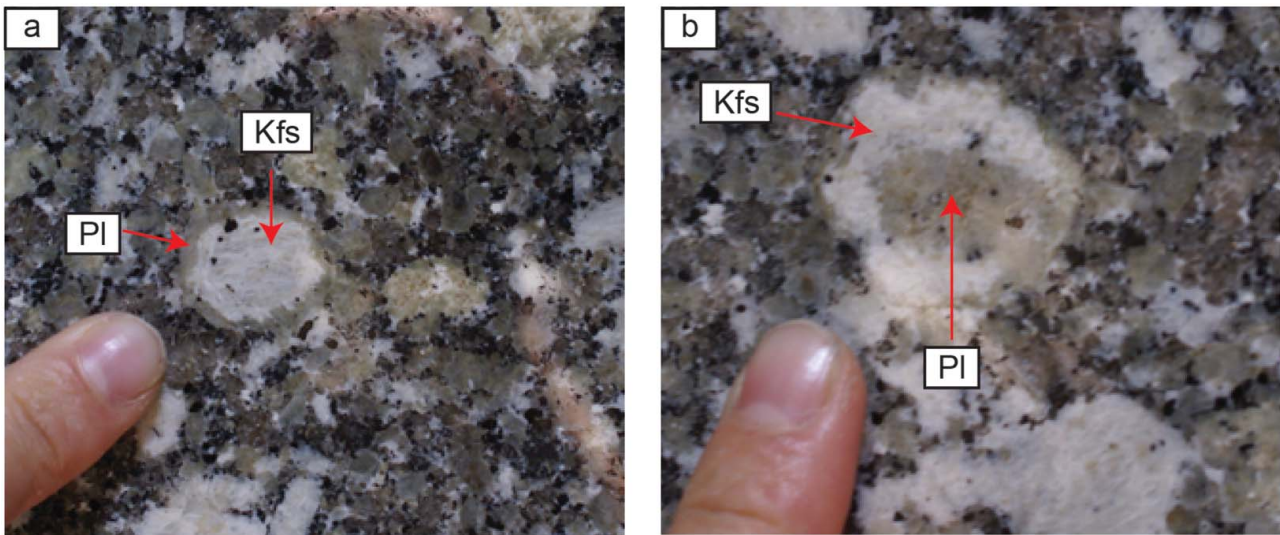


Figure 6. (a) Rapakivi (Kfs rimmed by Pl); and (b) antirapakivi (Pl rimmed by Kfs) textures in granodiorite, Tynong North Quarry (38°03'31"S, 145°37'22"E), Tynong pluton.

dilution are  $\pm 0.5\%$  and  $\pm 0.2\%$ , respectively. Isotope dilution analysis of US Geological Survey basalt standard BCR-2 yielded 46.5 ppm Rb, 338.2 ppm Sr,  $^{87}\text{Rb}/^{86}\text{Sr}$  0.398,  $^{87}\text{Sr}/^{86}\text{Sr}$  0.705001, 6.47 ppm Sm, 28.30 ppm Nd,  $^{147}\text{Sm}/^{144}\text{Nd}$  0.1381 and  $^{143}\text{Nd}/^{144}\text{Nd}$  0.512634. Long-term averages ( $\pm 2\text{SD}$ ) for  $^{87}\text{Sr}/^{86}\text{Sr}$  and  $^{143}\text{Nd}/^{144}\text{Nd}$  in BCR-2 and BHVO-2 are  $0.704996 \pm 51$  ( $n = 47$ ) and  $0.512641 \pm 24$  ( $n = 74$ ), and  $0.512998 \pm 25$  ( $n = 35$ ) and  $0.703454 \pm 43$  ( $n = 15$ ), consistent with reference values.  $\epsilon_{\text{Nd}}$  values were calculated using the modern CHUR parameters of Jacobsen and Wasserburg (1984) ( $^{147}\text{Sm}/^{144}\text{Nd} = 0.1967$ ,  $^{143}\text{Nd}/^{144}\text{Nd} = 0.512638$ ). Nd model ages ( $T_{\text{DM}-2}$ ) are two-stage model ages calculated for a modern depleted mantle with  $^{147}\text{Sm}/^{144}\text{Nd} = 0.2136$  and  $^{143}\text{Nd}/^{144}\text{Nd} = 0.513151$ ; a default average crustal  $^{147}\text{Sm}/^{144}\text{Nd} = 0.1100$  is used for the older stage. Decay constants are:  $^{87}\text{Rb}$   $1.397 \times 10^{-11}/\text{yr}$ ;  $^{147}\text{Sm}$   $6.54 \times 10^{-12}/\text{yr}$ .

Hf isotope ratios in magmatic (non-inherited) zircons were determined by laser ablation MC-ICP-MS at the University of Melbourne, using a HelEx 193 nm excimer laser system and Nu-Plasma MC-ICP-MS (Medlin et al., 2014; Woodhead, Hergt, Shelley, Eggins, & Kemp, 2004). Hf analytical sites were placed next to U–Pb analytical sites on grains that were large enough to do so and showed no textural evidence for inheritance on SEM images and in U–Pb isotope analyses (with some exceptions). A  $50 \mu\text{m}$  laser spot and 5 Hz repetition rate were used throughout, producing total Hf signals of 2–10 V at the start of the ablation.  $^{176}\text{Hf}/^{177}\text{Hf}$  ratios are corrected for Yb–Lu interferences and instrumental mass bias (normalisation to  $^{178}\text{Hf}/^{177}\text{Hf} = 0.7325$ ), and final results are reported relative to the accepted  $^{176}\text{Hf}/^{177}\text{Hf}$  ratios of standard zircons BR266 and 91500 (Woodhead & Hergt, 2005; Woodhead et al., 2004).  $^{176}\text{Lu}/^{177}\text{Hf}$  ratios were determined by reference to count rates on zircon standards with Lu/Hf known from isotope dilution analyses of bulk grains (Woodhead & Hergt, 2005).  $\epsilon_{\text{Hf}}$  values were calculated using the modern CHUR parameters of Blichert-Toft and Albarede (1997;  $^{176}\text{Lu}/^{177}\text{Hf} =$

$0.0332$ ,  $^{176}\text{Hf}/^{177}\text{Hf} = 0.282772$ ).  $T_{\text{DM}2}$  is a two-stage Lu–Hf depleted mantle model age based on a model depleted mantle with present-day  $^{176}\text{Lu}/^{177}\text{Hf} = 0.03829$  and  $^{176}\text{Hf}/^{177}\text{Hf} = 0.283224$  (equivalent to  $\epsilon_{\text{Hf}} = +16$  in average modern mid-ocean ridge basalt (MORB)) and a default crustal  $^{176}\text{Lu}/^{177}\text{Hf}$  of 0.0142, equivalent to the bulk crustal average Lu/Hf = 0.1 of Taylor (1985). Results for standard zircons 91500, BR266 and Temora collected during the two Hf analytical sessions were consistent with published reference values. Based on these results, analytical reproducibility for a homogeneous zircon is estimated to be in the range of  $\pm 1.5$  to  $2.5 \epsilon_{\text{Hf}}$  units. The Lu decay constant is  $1.865 \times 10^{-11}/\text{yr}$ .

## Results

### Major- and trace-element geochemistry

Major- and trace-element data for granitoids and enclaves are presented in the Supplementary Papers Table 3. Rock types range from hornblende-tonalite to biotite-leucogranite and all plutons are dominantly metaluminous ( $A/\text{CNK} < 1$ ), with the Tanjil Bren and Tynong bodies extending to slightly peraluminous compositions ( $A/\text{CNK} > 1$ ). Toorongu, Lysterfield and Baw Baw are compositionally similar, with silica contents between 63.3 and  $\sim 68$  wt%, while the Tynong and Tanjil Bren intrusions are more felsic, reaching 77.4 wt%  $\text{SiO}_2$ . Concentrations of Fe (as  $\text{Fe}_2\text{O}_3$ ), MgO, CaO,  $\text{TiO}_2$  and  $\text{P}_2\text{O}_5$  for the entire data set show well-defined to diffuse linear inverse correlations against  $\text{SiO}_2$ , whereas  $\text{K}_2\text{O}$  and ASI are positively correlated with  $\text{SiO}_2$  (Figure 7). By contrast,  $\text{Al}_2\text{O}_3$  and  $\text{Na}_2\text{O}$  show more diffuse and variable trends.

Microgranitoid enclaves and dioritic rocks from Lysterfield, Baw Baw and Tynong are metaluminous ( $A/\text{CNK}$  0.66–0.90) and have lower  $\text{SiO}_2$  (54.2–61.4 wt%) and higher Fe–Mg–Ca–Ti contents than the granites, and compositions are more scattered (Figure 7).  $\text{Na}_2\text{O}/\text{K}_2\text{O}$  tends to be higher

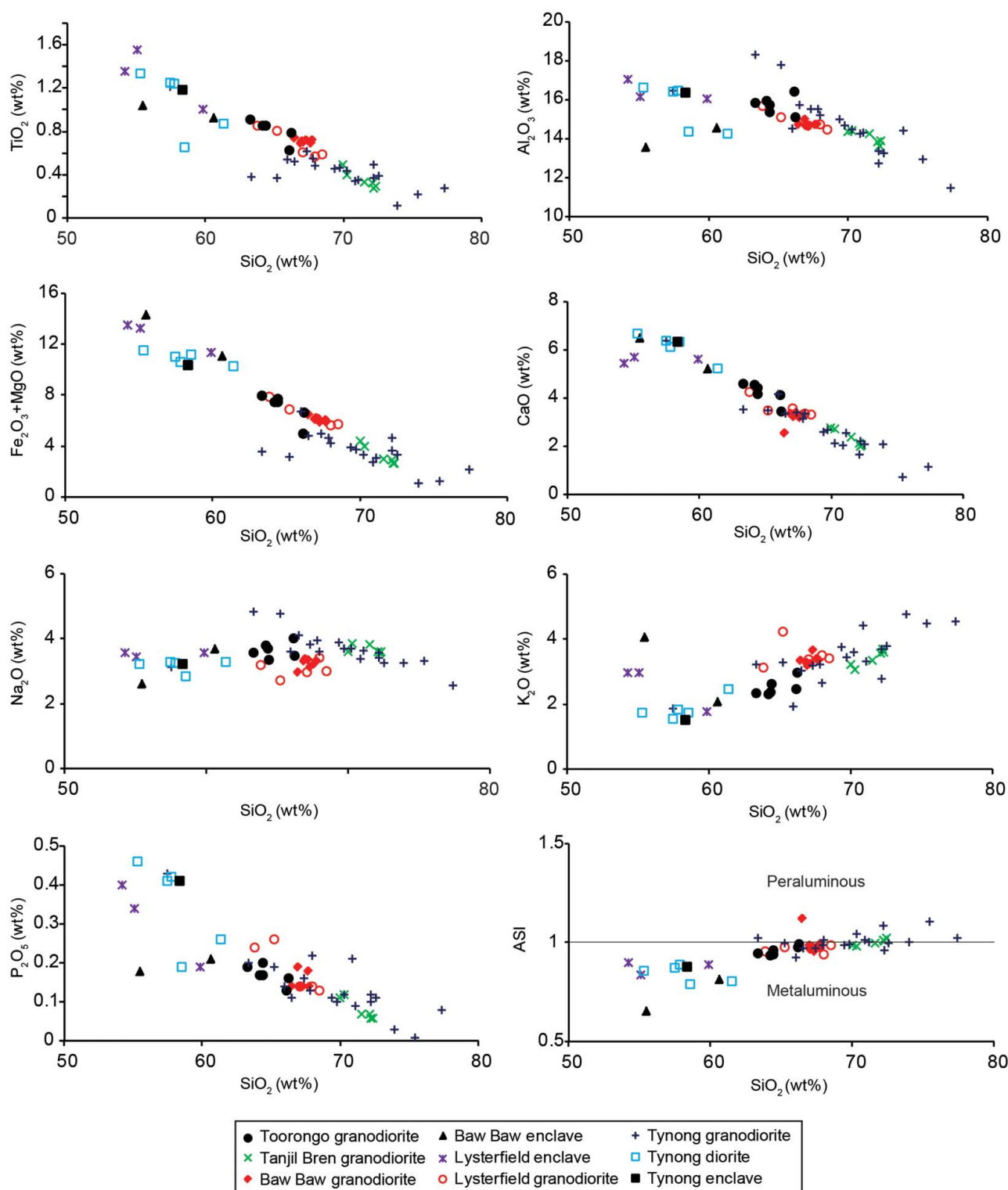


Figure 7. Harker diagrams for the Tynong Province granitoids.

(0.65–2.10, average  $1.60 \pm 0.44$ , 1SD) than in the granite host rocks (0.50–1.85, average  $1.02 \pm 0.35$ ), yet some of the enclaves have anomalously high  $K_2O$  (e.g. Baw Baw 304-1-1, 4.08 wt%  $K_2O$  @55.45 wt%  $SiO_2$ ), and this is reflected in high biotite content (e.g. Clemens et al., 2016).

Trace-element concentrations generally correlate poorly with major elements (Figure 8). Exceptions are Sr and Ga which are inversely correlated with silica, while Zr shows a more diffuse negative correlation. Rubidium, Pb and to a lesser extent Th and U, show positive linear correlations with

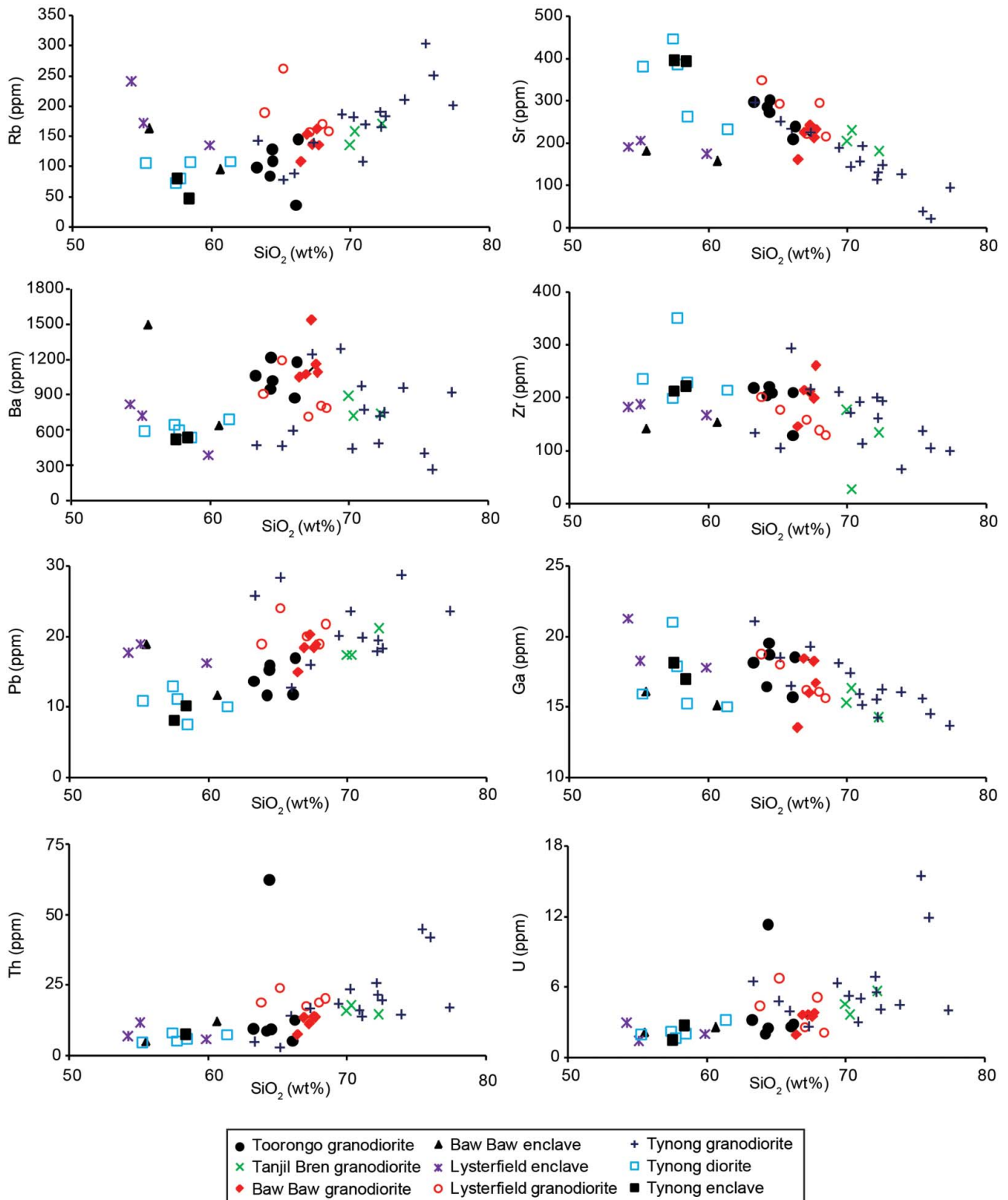


Figure 8. Selected trace-element patterns vs silica for the Tynong Province granitoids.

$\text{SiO}_2$ , whereas Ba shows a broad scatter. Likewise, trace-element concentrations in the enclaves and dioritic rocks are poorly correlated with major elements; only Th and U show well-defined correlations with  $\text{SiO}_2$  (Figure 8), as does V (not shown). High MgO contents (2.9–5.2 wt%) in enclaves and

diorites are associated with high and variable Ni–Cr contents, with particularly high Ni (up to 250 ppm) and Cr (up to 350 ppm) in two diorites and a hybrid granodiorite from the Tynong North Quarry locality. These samples may represent a distinct magma that could be derived from a mafic

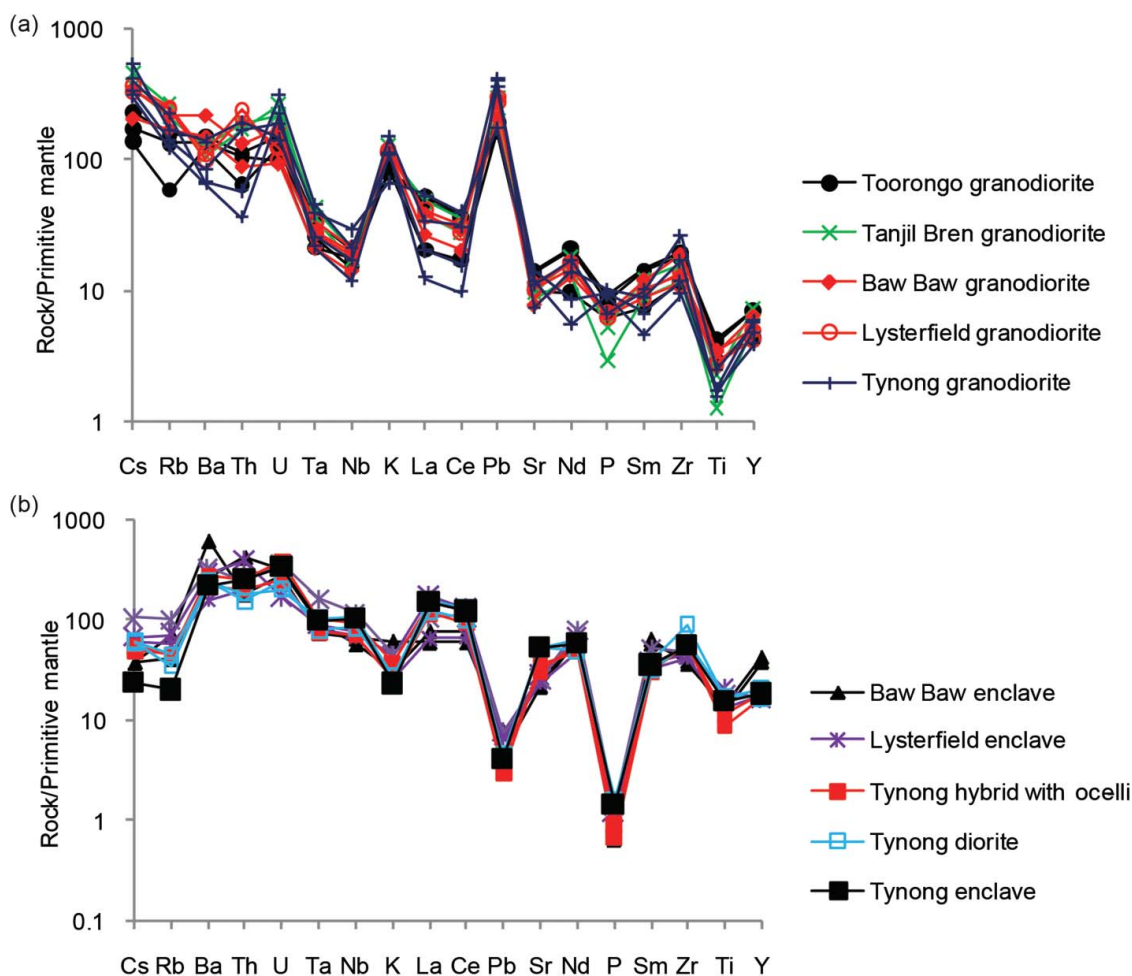


Figure 9. (a) Granitoid trace-element compositions normalised to Primitive Mantle values (Sun & McDonough, 1989); and (b) normalised patterns for enclaves and diorites.

(metabasaltic) source or result from hybridisation between mantle and crustal magmas (see also Clemens et al., 2016). Ba concentrations tend to be high in all samples (Figure 8), a well-known characteristic of the Late Devonian felsic magmatism in the Melbourne Zone (Rossiter & Gray, 2008). Two samples of the Baw Baw pluton (304-1-1 and 305-1) have very high Y contents (up to 70 ppm) that are consistent with their high levels of heavy rare earth elements (HREE).

Incompatible trace-element patterns in all analysed host granitoid samples are broadly similar and show negative anomalies for Ta, Nb, Sr and Ti and positive anomalies for U, K, Pb, Nd and Zr; the felsic Tanjil Bren pluton shows prominent depletion in P (Figure 9a). The enclaves, diorites and hybrids differ from the granitoids in having less depletion in Ta, Nb, Sr and Ti, but greater depletion in Cs, Rb, K and especially Pb and P; the biotite-rich enclave Baw Baw 304-1-1 shows relative enrichment in Ba and K (Figure 9b).

#### Rare earth elements (REE)

Rare earth concentrations in the granitoids vary widely (La  $\sim$ 30–110, Lu  $\sim$ 8–20 times chondritic), mirroring the wide ranges in SiO<sub>2</sub> and MgO. However, REE patterns are similar for

all granitic samples (Figure 10a, c), with La<sub>N</sub>/Sm<sub>N</sub> of 3 to 5 and flat HREE (Gd<sub>N</sub>/Lu<sub>N</sub>  $\sim$ 1–2). Most samples show pronounced Eu depletions although there are several examples without Eu anomalies. Samples 2803-5 and 2803-6 from the Tynong granodiorite have pronounced positive Eu anomalies, low total rare earth elements (REE) and low light REE levels (Figure 10a). These samples are enriched in Al<sub>2</sub>O<sub>3</sub> and Na<sub>2</sub>O compared with other Tynong granitoid samples, possibly reflecting Na-plagioclase accumulation.

The enclaves and dioritic rocks show greater diversity in REE patterns than their host rocks (Figure 10b). The two analysed enclaves from the Baw Baw Granodiorite have almost flat patterns while all other enclaves, and the Tynong North diorites and hybrids, show variable LREE enrichment (La<sub>N</sub>/Sm<sub>N</sub> = 1.9–4.5) and almost flat HREE (Gd<sub>N</sub>/Lu<sub>N</sub> = 1.4–1.9; Figure 10b). Eu/Eu\* varies from strongly negative in the enclaves from Baw Baw through slightly negative in the Lysterfield enclaves and to absent or weak in the Tynong pluton enclaves, diorites and hybrids. Despite their mafic–intermediate compositions, the dioritic rocks (enclaves + diorites) from the Tynong plutons have higher LREE concentrations than the host granitoids, whereas HREE concentrations are similar (Figure 10c).

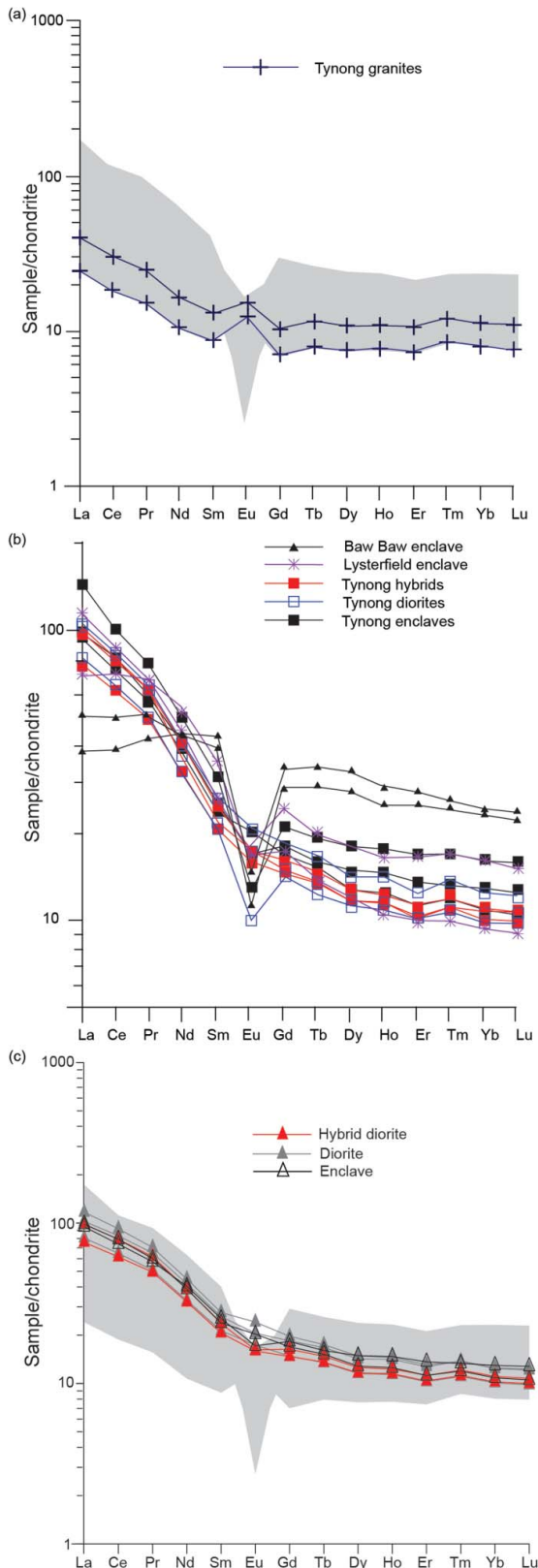


**Figure 10.** Chondrite normalised REE patterns for the Tynong Batholith granitoids, enclaves and coeval dioritic rocks: (a) the shaded field shows the range of REE patterns for all granitoids only (excluding enclaves and diorites). It is bounded by patterns for the extremes of Tynong pluton compositions. The patterns for two Tynong granitoids are superimposed to highlight their positive Eu anomalies; (b) REE patterns for dioritic rocks of the Baw Baw, Lysterfield and Tynong plutons; and (c) REE patterns for dioritic rocks of the Tynong pluton only, with the shaded field from (a) shown again for comparison. Normalising values from Taylor and McLennan (1995).

### Zircon U–Pb dating

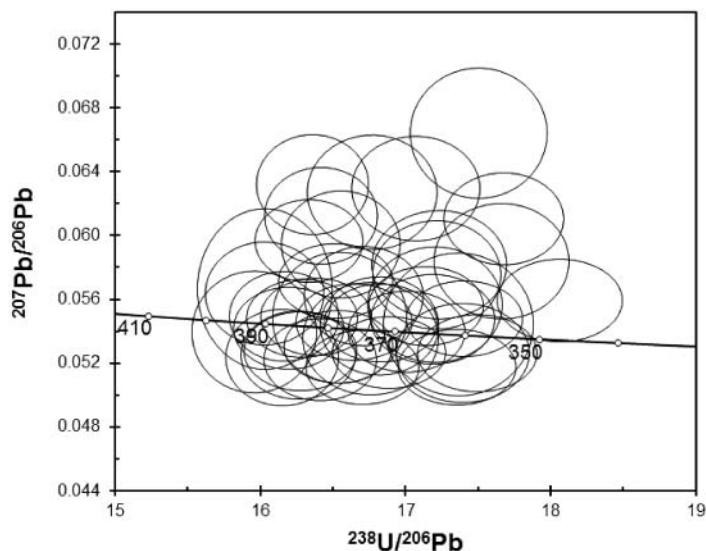
Zircons extracted from sample 406 (Toorongo granodiorite) are clear to pale pink, mostly prismatic and euhedral, with aspect ratios of 1:2–1:5. CL images show that the vast majority of grains are finely zoned, indicating a probable magmatic origin. Only a few grains have obvious inherited cores. Zircons in sample TYN5 (Tynong granodiorite) are generally similar; once more, textural evidence for possibly inherited cores is very rare.

The U–Pb isotope results (Supplementary Papers Tables 1, 2) are summarised in Tera Wasserburg diagrams (Figure 11). Most data points for sample 406 cluster near 370 Ma, producing a weighted average  $^{206}\text{Pb}/^{238}\text{U}$  ( $^{207}\text{Pb}$  corrected) age of  $372 \pm 3.4$  Ma [ $n = 42$ , with mean square weighted deviation (MSWD) = 1.09 calculated based on individual spot uncertainties derived by combining the internal and external precision by quadratic addition;  $2\sigma$ ], and this is considered to be the best estimate for magmatic crystallisation in this sample. Four additional ablations yielded Pb/U ages between 510 and 402 Ma that are interpreted as inherited ages (Supplementary Papers Table 1). Likewise, data points for sample TYN5 cluster in the range 370–360 Ma and yield a weighted average  $^{206}\text{Pb}/^{238}\text{U}$  ( $^{207}\text{Pb}$  corrected) age of  $362 \pm 9$  Ma ( $n = 20$ , with MSWD = 2.9 calculated as explained above;  $2\sigma$ ). Several data points were excluded owing to suspected Pb loss or excessive common Pb, yet both the error and MSWD of this average are high, suggesting potential complications in this data set. However, because all Pb/U ages that contribute to this average are for finely zoned, igneous zircons without obvious core structures, and its similarity to the known Late Devonian (370 Ma) age of the Tynong granodiorite, we interpret  $362 \pm 9$  Ma as the crystallisation age of this sample.

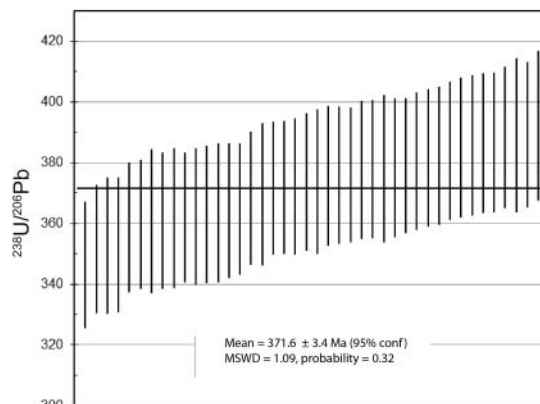
### Rb–Sr and Sm–Nd whole-rock isotopic systematics

New Sr–Nd isotope results for the Tynong, Toorongo, Baw Baw and Lysterfield granodiorites indicate initial  $^{87}\text{Sr}/^{86}\text{Sr} - \epsilon_{\text{Nd}}$  values (at 370 Ma) of 0.70557 to 0.70725 and  $-1.8$  to  $+0.7$  (Table 2). Nd model ages (2-stage depleted mantle model ages,  $T_{\text{DM}2}$ ) mirror the limited range in  $\epsilon_{\text{Nd}}$  and cluster near 1.1 Ga. Data for two microgranitoid enclaves (from Baw Baw and Lysterfield) are almost identical to those for their respective host rocks (Table 2), while the hybrid quartz diorite facies from the Tynong North locality shows slightly lower  $^{87}\text{Sr}/^{86}\text{Sr}$  and higher  $\epsilon_{\text{Nd}}$  than the three other Tynong samples in this data set. The data reported here are within the range of data reported in Maas and Nicholls (2012), Clemens and Bezuidenhout (2014) and Clemens et al. (2016) (Figure 12). The data set as a whole shows the expected inverse Sr–Nd isotope correlation from slightly positive  $\epsilon_{\text{Nd}}$  towards the more evolved  $\epsilon_{\text{Nd}}$  characteristic of the Paleozoic turbidites (e.g. Adams, Pankhurst, Maas, & Millar, 2005), which have been considered to be a possible crustal component in Lachlan Fold Belt granites (Keay et al., 1997). The data from the Tynong granodiorite have slightly higher  $^{87}\text{Sr}/^{86}\text{Sr}$  at a given  $\epsilon_{\text{Nd}}$  relative to other bodies (Figure 12). When combined

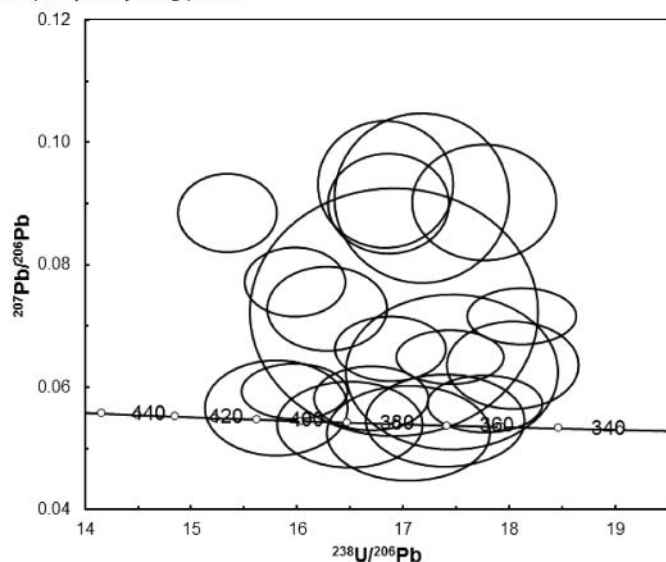
(a) Sample 406 Toorongo pluton



(b) Bar chart for sample 406



(c) Sample Tyn5, Tynong pluton



(d) Bar chart for sample TYN5

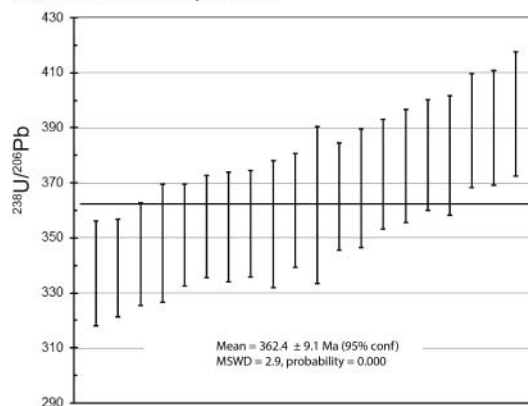
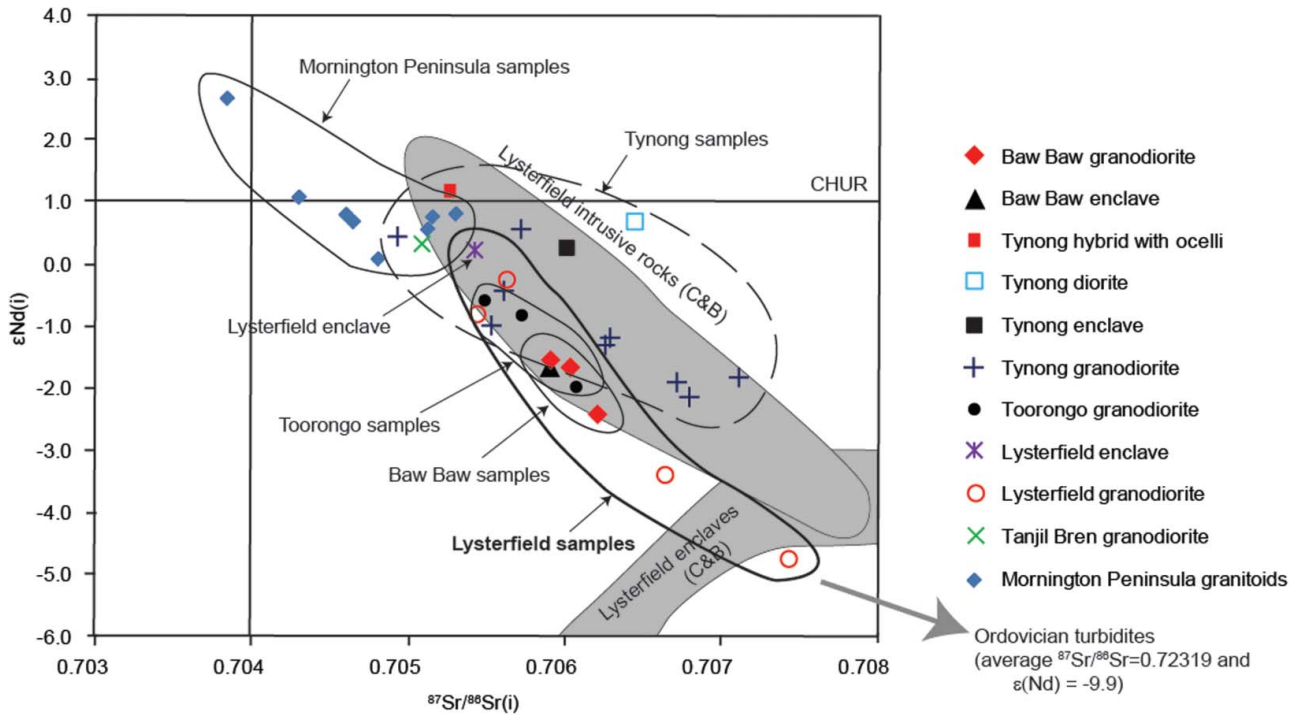


Figure 11. Tera-Wasserburg U–Pb isotope concordia diagrams for zircons: (a) Toorongo granodiorite (sample 406); and (b) Tynong granodiorite (sample TYN5). The weighted average,  $^{207}\text{Pb}$  corrected  $^{206}\text{Pb}/^{238}\text{U}$  ages are indicated. MSWD includes both the internal and external precisions, and all uncertainties are  $2\sigma$ . See Supplementary Papers Tables 1 and 2.

Table 2. Rb–Sr and Sm–Nd isotopic data for the Tynong Province granitoids. Age corrections were based on an average 370 Ma, the crystallisation age of plutons of the Tynong Province granitoids.

	304-1-1 Baw Baw enclave	306 Baw Baw granodiorite	2802-3 Tynong hybrid	2803-10 Tynong diorite	2803-5 Tynong granodiorite	2803-8 Tynong granodiorite	403 Toorongo granodiorite	406 Toorongo granodiorite	1702-4 Lysterfield enclave	1702-1 Lysterfield granodiorite
Rb ppm	167.0	150.0	102.9	113.1	160.3	71.4	98.5	96.6	239.6	156.9
Sr ppm	184.4	201.5	256.1	411.4	304.3	391.5	321.9	315.2	250.4	286.1
$^{87}\text{Rb}/^{86}\text{Sr}$	2.623	2.155	1.163	0.795	1.525	0.527	0.886	0.887	2.771	1.587
$^{87}\text{Sr}/^{86}\text{Sr}$	0.71972	0.71726	0.71139	0.71063	0.71515	0.70848	0.71016	0.71039	0.72003	0.71399
Sm ppm	9.22	5.19	4.84	5.21	3.19	5.71	6.14	4.92	8.11	4.75
Nd ppm	28.33	21.89	24.33	26.63	13.17	29.78	28.89	24.95	37.76	25.13
$^{147}\text{Sm}/^{144}\text{Nd}$	0.1964	0.1432	0.1200	0.1181	0.1462	0.1159	0.1283	0.1190	0.1297	0.1142
$^{143}\text{Nd}/^{144}\text{Nd}$	0.512552	0.51243	0.512514	0.512483	0.512423	0.512471	0.512444	0.512408	0.512488	0.512426
$\epsilon_{\text{Nd}}$ meas	−1.68	−4.06	−2.42	−3.02	−4.19	−3.26	−3.78	−4.49	−2.93	−4.14
$T_{\text{DM2}}, \text{Ga}$	1.19	1.18	0.97	1.01	1.20	1.02	1.10	1.12	1.05	1.08
$^{87}\text{Sr}/^{86}\text{Sr}(t)$	0.70613	0.70609	0.70536	0.70651	0.70725	0.70575	0.70557	0.70579	0.70567	0.70576
$\epsilon_{\text{Nd}}(t)$	−1.7	−1.5	1.2	0.7	−1.8	0.6	−0.6	−0.8	0.2	−0.2



**Figure 12.**  $\epsilon_{\text{Nd}(i)}$  vs  $^{87}\text{Sr}/^{86}\text{Sr}(i)$  plot for igneous rocks from the Tynong Batholith and Mornington Peninsula granitoids. Note the primitive nature of the Tynong quartz diorite with ocelli (Tynong hybrid), comparable with those of the Mornington Peninsula granitoids. Data for the Tynong Province are given in Table 2. Data for Ordovician turbidites from McCulloch and Woodhead (1993). Grey fields correspond to Lysterfield samples from Clemens and Bezuidenhout (2014) divided into enclaves and main intrusive body.

with the data for Late Devonian granites from the Mornington Peninsula (Tzikas, 2002), the Tynong granodiorite data could be interpreted as a separate trend to Baw Baw, Toorong and Lysterfield granodiorite trends (Figure 12).

### Hf isotopes

Hf isotope ratios were obtained for intrusion-age zircons in samples TYN5 and 406, from the Tynong and Toorong granodiorites, respectively. Additional data were obtained for zircons in sample 2803-8, from the Tynong granodiorite, which contains zircons that are virtually identical to those in the other two samples, in both internal structure and U–Pb age systematics (Figure 13; Regmi, 2013). Initial  $\epsilon_{\text{Hf}}$  values were calculated at 370 Ma, the generally accepted emplacement age of the Tynong Province plutons, and confirmed by our own U–Pb zircon dating.

Zircons from sample TYN5 yield initial  $^{176}\text{Hf}/^{177}\text{Hf}$  from 0.282519 to 0.282805 (Supplementary Papers Table 4), equivalent to  $\epsilon_{\text{Hf}(i)}$  from  $-0.8$  to  $+9.3$ , with an average of  $+4.3 \pm 4.2$  ( $n = 34$ , 2SD). Zircons from sample 2803-8 yield initial  $^{176}\text{Hf}/^{177}\text{Hf}$  from 0.282665 to 0.282790 and  $\epsilon_{\text{Hf}(i)}$  from  $+4.3$  to  $+8.8$ , with an average of  $+6.9 \pm 2.3$  ( $n = 23$ , 2SD). Initial  $^{176}\text{Hf}/^{177}\text{Hf}$  in zircons from sample 406 vary from 0.282512 to 0.282762 and corresponding  $\epsilon_{\text{Hf}(i)}$  values from  $-1.1$  to  $+7.8$ , with an average of  $+3.9 \pm 4.1$  ( $n = 17$ , 2SD). Hf model ages ( $T_{\text{DM}2}$ ) for the three samples average 1.22 Ga (TYN5), 0.86 Ga (2803-8) and 1.05 Ga (406), and are similar to their whole-rock Nd model ages ( $T_{\text{DM}2}$ , 1.22 Ga, 1.02 Ga, 1.12 Ga), respectively;

Nd isotope information for TYN5 from Maas & Nicholls, unpubl. data).

The range in zircon  $\epsilon_{\text{Hf}}$  for sample 2803-8 (4.5 units total range) is consistent with the external precision of our *in situ* Hf isotope analyses. By contrast, the  $\epsilon_{\text{Hf}}$  ranges for zircons from samples TYN5 (10.1 units) and 406 (8.9 units) exceed those expected from analytical error alone, by factors 2–2.5. The lowest  $\epsilon_{\text{Hf}370}$  values (grain TYN5.22,  $\epsilon_{\text{Hf}} = -0.8$ ; grain

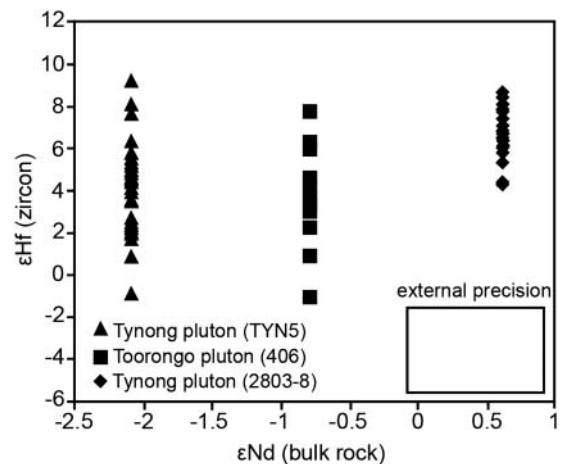


**Figure 13.**  $\epsilon_{\text{Nd}(i)}$  (whole rock) vs  $\epsilon_{\text{Hf}}$  (zircon) for the Tynong and Toorong plutons. Note the more mantle-like character of the  $\epsilon_{\text{Hf}}$  signature and  $\epsilon_{\text{Nd}(i)}$  of the Tynong sample 2803-8. Sample TYN5, despite having the most negative  $\epsilon_{\text{Nd}(i)}$  value, has  $\epsilon_{\text{Hf}}$  values that cover the entire range of the other two samples (see Supplementary Papers Table 4). The rectangle on the lower right indicates the value of the external precision for  $\epsilon_{\text{Hf}}$  ( $\pm 2$  units) and  $\epsilon_{\text{Nd}(i)}$  ( $\pm 0.5$  units).

406.13,  $\varepsilon_{\text{Hf}} = -1.1$ ) are on rare grains. If these data points were excluded, the  $\varepsilon_{\text{Hf}}$  ranges are reduced to 8.3 units (TYN5) and 6.8 units (sample 406), still greater than the external precision. Several zircon grains in TYN5 were large enough for two Hf analytical spots. One of them shows significant internal variation (6.9 units, grain TYN5.24), and the other five examples show within-grain variation of  $\leq 4.3$  units. Although most of these within-grain isotopic ranges are small, it is interesting to note that all but one have a higher  $\varepsilon_{\text{Hf}}$  in the middle of the grain than in their outer parts. Unless there are unrecognised age variations (inherited cores) within these grains, these data suggest a small degree of syn-magmatic heterogeneity in the  $^{176}\text{Hf}/^{177}\text{Hf}$  recorded in these zircons.

## Discussion

### Major-element variations: PAE or mixing?

Linear compositional trends in granitoid series have been used to argue for various mixing (or unmixing) mechanisms. The near-linear variations for  $\text{Fe}_2\text{O}_3$ , MgO, CaO,  $\text{TiO}_2$  and ASI in Tynong Province I-type granites reported here (Figure 7) could be interpreted to result from magma mixing or wall-rock assimilation (Wall et al., 1987), PAE (Clemens & Stevens, 2012), restite unmixing (e.g. Chappell et al., 1987), crystal fractionation (e.g. Sawka, Heizler, Kistler, & Chappell, 1990), or a combination of these.

A dominant role for magma source variation was favoured by Clemens and co-authors, who observed that samples in the range 60–65 wt%  $\text{SiO}_2$  are scarce within the compositional spectrum of the Tynong granodiorite; readily verified from the data shown in Figure 7. By contrast, no such gap appears to exist in the Lysterfield granodiorite (Figure 7; see also Clemens & Bezuidenhout, 2014; Clemens et al., 2016). Although sampling issues cannot be excluded, these authors interpreted the compositional gap in the Tynong intrusion data as marking the difference between two magma batches that evolved separately (Clemens et al., 2016): a mafic–intermediate magma and an I-type, low-Al intermediate–felsic magma series, thought to be derived from melting of immature greywackes located within the mid-to lower-crustal Selwyn Block. There may have been a number of different sources for the crustal I-type granitoids. For example, the high- and low-Al groups defined for the Tynong pluton (Clemens et al., 2016) could be melts derived from different crustal sources, one richer in muscovite, or from sources that had restitic and/or peritectic hornblende left in the source. Such differences could explain some of the isotopic differences between samples.

While the presence of multi-scale hybridisation features (hybrid zones in the Tynong North Quarry, enclaves, ocelli, rapakivi textures) strongly indicate that magma mixing played a role in the origin of the Tynong Province plutons, Clemens et al. (2016, figure 10) observe that an extrapolation of  $\text{Al}_2\text{O}_3$ – $\text{Na}_2\text{O}$  systematics in the Tynong granodiorite does not pass through the compositions of typical calc-alkaline basalts and argue that this rules out mafic–felsic magma mixing as a

major control on chemical variability in the two compositional groupings of the Tynong granodiorite. However, apart from the possibility that mixing processes could be complex (e.g. de Campos, Perugini, Ertel-Ingrisch, Dingwell, & Poli, 2011; Perugini & Poli, 2012; Ubide et al., 2014), the use of Al–Na elemental systematics to trace potential basaltic/andesitic mixing components is problematic. Like many granite suites, the Tynong Province granitoids, hybrids, diorites and enclaves show diffuse or non-linear trends for  $\text{Al}_2\text{O}_3$ ,  $\text{Na}_2\text{O}$  and  $\text{K}_2\text{O}$  against  $\text{SiO}_2$  (Figure 7) and this possibly reflects complexities resulting from magma flow and high alkali–Al diffusivity in magmas (Acosta-Vigil, London, & Morgan, 2012). Late-magmatic redistribution of highly differentiated interstitial, alkali-rich melt and/or hydrothermal fluids will add further complexity and suggests that Al–alkali systematics are not ideal to investigate magma mixing.

### PAE

Clemens and Stevens (2012) set out a number of deficiencies that they perceive in the models used to explain chemical variation within granitic suites, such as magma mixing, crystal fractionation, restite unmixing, progressive partial melting and wall-rock assimilation. They propose that a PAE model could account for much of the variation seen in both I- and S-type magmatic rocks of the Tynong Province rocks. The PAE model proposes that upon withdrawal from its source, a felsic crustal melt carries only small grains and that the only grains that are sufficiently small are exclusively peritectic phases and some accessory phases. The relative proportions of peritectic phases, dictated by the stoichiometry of the melting reactions are proposed to remain fixed during magma transport (Clemens & Stevens, 2012). They argue that such assemblages, and their fate during transport of the host melt, have a strong control on the chemical character and evolution of the resulting magma bodies and suggest that PAE accounts for much of the (typically linear) compositional variation seen in both I- and S-type magmatic suites such as the Tynong Province granitoids (Clemens et al., 2016).

Despite being co-authors in one of the papers cited above (Clemens et al., 2016), we have reason to think that multi-step magma mixing processes might be a more robust explanation for the chemical variation in the Tynong Province. Before outlining a model based on magma mixing, we first discuss some of the possible deficiencies of the PAE model: (a) assumptions regarding the size and nature of channel networks draining the magma source, (b) the possible implications of differences in grain size and growth rates of the various peritectic minerals, (c) the assumption of fixed proportions of peritectic phases in the draining melt, and (d) the need for an exception to the ‘small crystals’ rule to allow the transport of large peritectic plagioclase crystals.

An implicit assumption of the PAE model is that melt is drained from the source by an interconnected network of narrow channels (point (a) above) that never become wide enough to allow passage of non-peritectic residual grains, and also that the network never becomes voluminous

enough to disrupt the source region. While this may arguably be the case in some terranes, there are numerous examples of migmatites where melt has disaggregated the source and carried residual minerals in various proportions. This is true for both water-fluxed and dehydration melting terranes alike, where the nature of the extraction network is a function of the ratio between the rate of melt production and that of melt extraction, and also a function of rock strength and anisotropy, and the differential stresses and pressure gradients driving magma migration, to name a few variables.

Points (b) and (c) relate to the ability of melt to carry peritectic minerals. Different peritectic minerals growing simultaneously have considerably different physical properties and preferred growth locations (some peritectic minerals grow preferentially in the leucosome, others in the melanosome of migmatites). Why would these minerals be equally dragged into the melt and carried in equal and fixed proportions when their physical properties are so different even during the very first growth stages? A compounding difficulty is how to avoid carrying any small grains of the reactant phases within the melt. Reactants decrease in grain size during melting and could easily be incorporated.

Variations in CaO related to PAE are believed to be a result of entrainment of plagioclase (point d). In order to keep the model consistent, its proponents suggest that only peritectic plagioclase is entrained. In some cases, these can be relatively large grains (3 mm for the Lysterfield granite; Clemens & Bezuidenhout 2014). In this case, the authors argue that given the low density of plagioclase and its involvement in melting as a reactant to release Na<sub>2</sub>O, peritectic grains will form in the vicinity of the melt making them 'texturally predisposed to entrainment' (Clemens & Stevens, 2012). This however is true also for the other main reactants, such as quartz, K-feldspar or even non-peritectic plagioclase, so why can only the peritectic grains be carried?

The assumptions underlying PAE contradict the well-documented nature of anatectic terranes, in which disruption and transport of all residual minerals by the magma are the norm, not the exception. Chappell (1987) defined restite unmixing as the mobilisation of the source rock by anatexis to form a magma, and subsequent differentiation by gradual separation of the restite (including both primary minerals and peritectic minerals). If we relax the rules of both these processes (PAE and restite unmixing), we have an appropriate description of magma extraction. Migmatite terranes typically record the partial disruption of the source, not necessarily the full mobilisation required by Chappell and coworkers, and the transport of all kinds and sizes of residual minerals, not the preferential transport of peritectic minerals.

#### **Possible additional controls on magma compositions: trace-element evidence**

Source composition exerts a strong control on the chemistry of crustal magmas. The high Ba contents typical of the Tynong Province are common to all Late Devonian felsic complexes in the Melbourne Zone and therefore clearly a feature

of the magma source (Rossiter & Gray, 2008). Other possible source features are less distinctive. For example, high Rb and Pb contents in the Lysterfield and Baw Baw plutons may reflect abundant alkali feldspar phenocrysts in the granite or source rocks rich in muscovite. All Tynong Province granitoids have very similar incompatible trace-element patterns, characterised by depletion of Nb, Ta, Sr and Ti typical of most crustal magmas, and the continental crust in general. Crustal contributions are also supported by the Sr–Nd isotopic data.

Fractional crystallisation processes are probably the reason for highly variable REE concentrations in Tynong Province granitoids (e.g. 9–39 ppm La), both within a single pluton (e.g. Tynong) and between plutons. Eu anomalies vary considerably, and some samples show evidence for plagioclase accumulation. An inverse correlation of Sr with SiO<sub>2</sub>, observed in many granite series and also in the Tynong Province may be due to plagioclase fractionation (Figure 8). Likewise, the anti-correlation of V with SiO<sub>2</sub> (see Supplementary Papers Table 3) may be related to fractionation of ilmenite, while high Y content in some samples from Baw Baw may be attributed to accumulation of clinopyroxene and amphibole.

An input of relatively unevolved more mafic magma is indicated by the presence of Mg-rich hybridised diorites (Tynong samples 2803-10, 2803-4 and 2803-2) with high Ni, Cr and Co. However, Cr–Ni concentrations in the microgranitoid enclaves are highly variable, with low Cr/Ni in the Lysterfield enclaves and high Cr/Ni in the Baw Baw enclaves (Supplementary Papers Table 3). This variability may reflect heterogeneous mixing of more mafic magmas to produce these broadly dioritic magma compositions, and/or intrinsic variation in the composition of these mafic magmas. The flat REE patterns and high HREE levels of the Baw Baw enclaves (Figure 10b) may be related to the accumulation of clinopyroxene and amphibole.

#### **Ages of the Tynong and the Toorong granodiorites**

Zircon U–Pb ages for the Tynong and Toorong granodiorites obtained by LA-ICP-MS ( $372 \pm 2$ ,  $362 \pm 9$  Ma, respectively) are consistent with the well-established age of the Late Devonian felsic magmatism of the Melbourne Zone (Vandenberg et al., 2000), such as  $374 \pm 2$ ,  $373 \pm 3$  and  $366 \pm 3$  Ma SHRIMP U–Pb zircon ages for the Strathbogie Batholith (Bierlein, Arne, Keay, & McNaughton, 2001, Kemp et al., 2008) or  $373 \pm 2$  and  $375 \pm 2$  Ma SHRIMP U–Pb zircon ages for felsic volcanics of the Cerberean Cauldron of the Yarra Ranges, immediately to the north of the Tynong Province (Compston, 2004). Rare inherited zircons have apparent ages between 510 and 400 Ma, similar to ages of inherited zircons in other Lachlan Orogen I-type granitoids and in their host metasedimentary rocks (Kemp et al., 2005).

#### **Isotopic constraints**

High average  $\epsilon_{\text{Hf}(t)}$  values recorded in magmatic zircon in the Tynong and Toorong granodiorites suggest their parent magmas were derived from relatively unevolved sources. The

differences between the three samples studied are not significant although the slightly higher zircon  $\epsilon_{\text{Hf}(t)}$  in the Tynong granodiorite ( $+6.9 \pm 2.3$  and  $+4.3 \pm 4.2$  vs  $+3.9 \pm 4.1$  in Toorongoo) correlates with subtly higher whole-rock  $\epsilon_{\text{Nd}}$  ( $-1.8$  to  $+1.2$  vs  $-0.8$  to  $-0.6$ ) for Tynong; initial  $^{87}\text{Sr}/^{86}\text{Sr}$  ratios are similar in both plutons. The Nd–Hf isotope data lie within the broad global Nd–Hf isotope trend and are isotopically similar to some modern oceanic basalts (oceanic arcs, ocean island basalt) but also to modern abyssal sediment and active margin basalts (e.g. Chauvel, Lewin, Carpentier, Arndt, & Marini, 2008; Vervoort, Patchett, Blichert-Toft, & Albarède, 1999). A magma source composed of old metabasalts, possibly with immature arc-derived and abyssal sediments, would be consistent with the isotopic and geochemical data. However, such interpretations are problematic if mixing (source or syn-magmatic) were involved. The zircon Hf isotope data appear to indicate some degree of Hf isotopic heterogeneity [ $\epsilon_{\text{Hf}(t)}$   $\sim +9$  to  $\sim +1$ ], consistent with a magma mixing model involving contrasting basic and silicic magmas (e.g. Kemp et al., 2007).

Tynong Province Sr–Nd isotopic compositions (0.7050–0.7075,  $\epsilon_{\text{Nd}}$  +0.4 to  $-4.7$ ), Figure 14 are similar to those in many other I-type granitoids of the Lachlan Fold Belt (e.g. McCulloch & Woodhead, 1993), including those from other complexes of the Melbourne Zone (e.g. Maas & Nicholls, 2012), and are consistent with magma sources that had a relatively brief crustal history ( $T_{\text{DM}}$  model ages *ca* 1 Ga) and were not involved in repeated sedimentary cycling that significantly increases Rb/Sr ratios and  $^{87}\text{Sr}/^{86}\text{Sr}$  initial ratios. The data show the broad inverse correlation (Figure 12) observed in numerous granitic provinces, including SE Australia (e.g. Keay et al., 1997; McCulloch & Chappell, 1982). Explanations for such correlations include source heterogeneity (Hergt, Woodhead, & Schofield, 2007; McCulloch & Chappell, 1982), assimilation/fractional crystallisation (Black et al., 2010), and crustal-scale hybridism (Gray, 1984, 1990; Keay et al., 1997). Hybridism models have also been examined for individual plutons (Eberz et al., 1990; Maas et al., 1997).

One of the potential outcomes of magma mixing/hybridism is correlated change in radiogenic isotope ratios and major (e.g.  $\text{SiO}_2$ , MgO) and trace (e.g. Cr, Ni) element concentrations, reflecting conservative mixing of distinct components (e.g. Carlson, Lugmair, & Macdougall, 1981). However, correlated changes of this type were not observed for Silurian I–S-type granites of the eastern Lachlan Fold Belt (McCulloch & Chappell, 1982; but also Gray, 1984, 1990) and are not obvious in the Tynong Province data (Figure 14). There is some correlation for subsets of the data, for example, the data for the Tynong granodiorite alone show broad correlations of  $\epsilon_{\text{Nd}}$  with Si, K, Na/K (positive) and with Ti, Fe, Mn, Mg, Ca (negative). These are the kinds of changes expected in mixing of mafic (low Si, K, high Mg, Fe, Ca, high  $\epsilon_{\text{Nd}}$ ) and felsic, crust-derived (high Si, K, low Mg, Fe, Ca, low  $\epsilon_{\text{Nd}}$ ) magmas in a conservative mixing regime, i.e. where the resulting mixtures are not greatly modified by further mixing with other components, or by fractional crystallisation (e.g. Gray, 1990). The important aspect here is that the correlations are best

developed for samples of host granodiorite, which represent an extensive (900 km<sup>2</sup>) outcrop area, while the enclaves and the lithologies from the Tynong North Quarry mixing zone show greater scatter. No equivalent correlations are seen for  $^{87}\text{Sr}/^{86}\text{Sr}$  in the Tynong data, or for the data from other plutons in the Tynong Province (although the data set as a whole shows a broad correlation of  $\epsilon_{\text{Nd}}$  with Na/K).

A lack of chemical–isotopic correlations could also be a result of protolith heterogeneity (McCulloch & Chappell, 1982) and the nature of melting reactions in protoliths of different mineralogy and composition (e.g. Clemens & Stevens, 2012). For example, decoupling of chemical (e.g.  $\text{SiO}_2$ ) and radiogenic isotope characteristics in the Lysterfield granodiorite (Figure 15) could be the result of solid entrainment (Clemens & Bezuidenhout, 2014). While we cannot rule out such alternatives, we propose that a lack of systematic variation between chemical and isotopic compositions expected in a generalised magma mixing model could be a result of multiple stages of magma mixing interspersed with periods of fractionation, assimilation or both. These stages could have occurred during magma genesis, transport and pluton assemblage. Early formed hybrid magmas fractionated and then interacted with other fractionated hybrid magmas. In a dynamic scenario of this type, mixing and mingling would occur between multiple and transient components.

### **Magma mixing/mingling**

Magma mixing and mingling have been used widely to explain the origin of the S-type and I-type granitoids of the Lachlan Fold Belt by a number of authors (Collins, 1996; Elburg & Nicholls, 1995; Keay et al., 1997; Kemp et al., 2007). In contrast, Chappell (1996), and more recently Clemens and Bezuidenhout (2014) and Clemens and Stevens (2012), argued that magma mixing cannot be a major process in granite petrogenesis in the Lachlan Fold Belt.

In the case of the Tynong Province granitoids, several lines of field and petrographic evidence suggest a major role of magma mingling/mixing processes. The presence of coeval, variably hybridised mafic–intermediate bodies (diorites and hybrid quartz diorites with plagioclase and quartz ocelli), especially in the Tynong North Quarry, suggests input of mafic–intermediate magmas. The hybrid quartz diorite itself represents different stages of interaction between mafic and felsic magmas. Based on their rounded or lobate shapes (Figure 4a, b) and their fine grain size, the microgranitoid enclaves are interpreted to represent chilled fragments of mafic, variously hybridised magma that crystallised rapidly in contact with the cooler, more silicic host magma (Hibbard, 1981; Wiebe, 1994). The mineralogy of the granitoids also indicates multiple components: the presence of clinopyroxene and hornblende and the dominantly metaluminous character of the rocks are consistent with an I-type character, yet the rocks also carry ilmenite as the Fe–Ti oxide and reddish brown Ti-rich,  $\text{Fe}^{3+}$ -poor biotite, the type of biotite that is typical of the reduced mineralogy of S-type granitoids (Chappell & White, 1992). Further, all Late Devonian granitoids

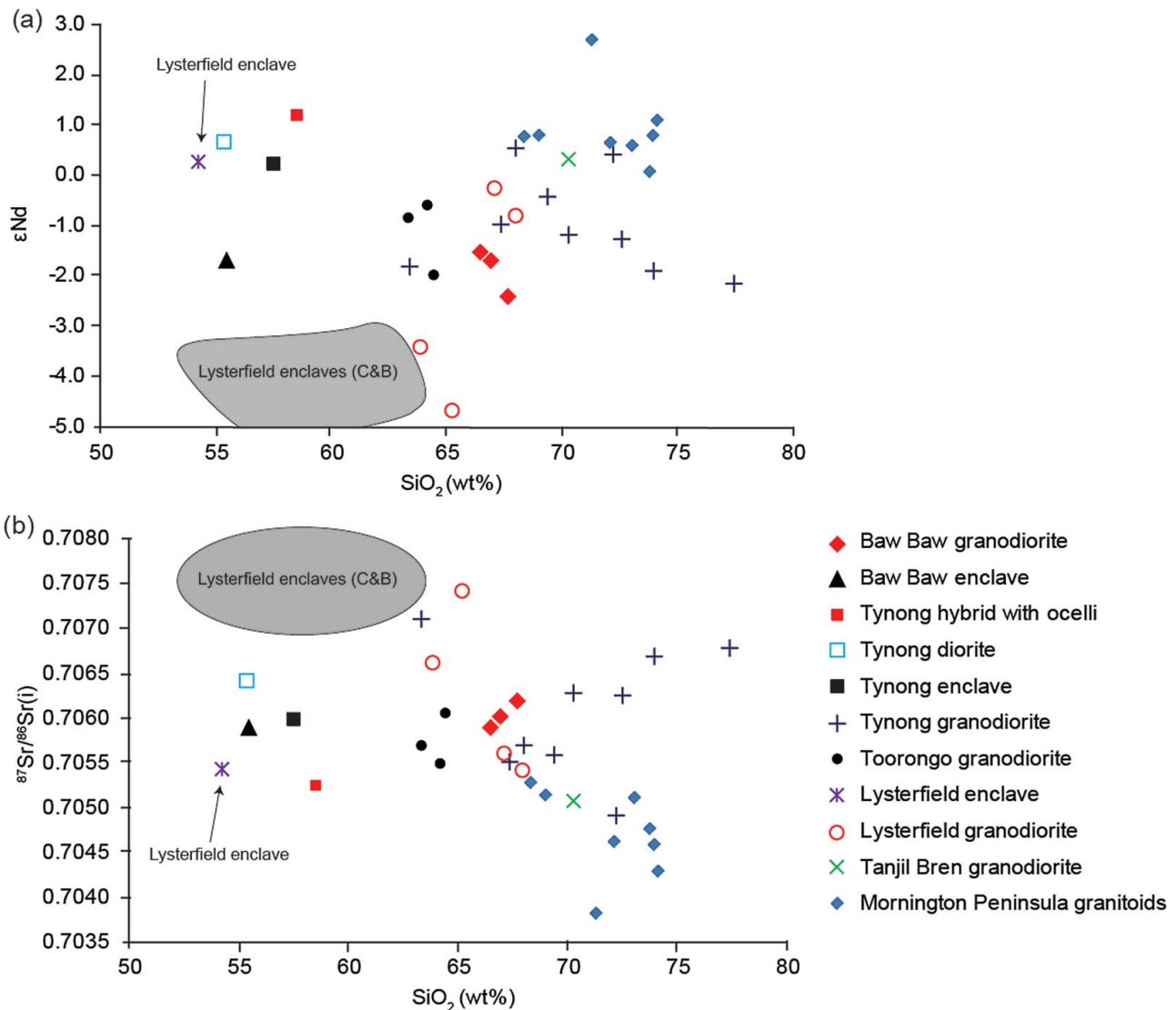


**Figure 14.** (a)  $\epsilon_{\text{Nd}(t)}$  vs  $\text{SiO}_2$  (wt%) plot for rocks from the Tynong Province lacking a clear trend and with a broad range of  $\epsilon_{\text{Nd}(t)}$  values for a given  $\text{SiO}_2$  value, typically over more than three  $\epsilon$  units. In particular, note the more primitive nature of the Tynong quartz diorite with ocelli (Tynong hybrid) in spite of being richer in  $\text{SiO}_2$  than some other samples. Data in Table 2 and unpublished data from Maas & Nicholls, and Tzikas (2002). (b)  $^{87}\text{Sr}/^{86}\text{Sr}(i)$  vs  $\text{SiO}_2$  (wt%) plot for rocks from Tynong Province lacking a clear trend.

(I- and S-type) and the coeval (overwhelmingly S-type) volcanic sequences of the Melbourne Zone have anomalously high Ba contents (>700 ppm in unfractionated granitoids; Rossiter, 2008), which presumably reflect a crustal (sedimentary?) component in the magma sources.

At the microscopic scale, magma mingling and partial hybridisation is supported by a number of mineral instability features. Rapakivi and antirapakivi textures may arise from a number of processes (Dempster, Jenkin, & Rogers, 1994; Eklund & Shebanov, 1999), one of which is magma mixing (Hibbard, 1981; Wark & Stimac, 1992). When magmas of contrasting composition mix, quenching of the more mafic magma may result in the epitaxial growth of plagioclase onto K-feldspar crystals derived from the more felsic magma. Grains of quartz and plagioclase rimmed by amphiboles (ocelli), well developed in the Tynong North Quarry, also suggest hybridisation and quenching (Hibbard, 1991; Vernon,

1990). The ocelli are formed by partial dissolution of mineral grains from the felsic magma entrained by the mafic magma. Dissolution extracts latent heat from the adjacent liquid and the undercooled surface of the xenocryst becomes a preferential nucleation substrate for amphiboles from the mafic magma (Palivcova, Waldhausrova, & Ledvincova, 1995). Experiments also suggest that the long prismatic, acicular apatite crystals (Figure 5) result from rapid cooling (Wyllie, Cox, & Biggar, 1962). These are common in microgranular enclaves worldwide, including those from the Tynong Province, and are interpreted to indicate a magma mingling setting (Hibbard, 1991).

The microscopic mafic clots commonly observed in granites, and cited as examples of modified restite (Chappell et al., 1987), have been interpreted as converted mineral aggregates from coeval mafic magma globules (Barbarin & Didier, 1992; Baxter & Feely, 2002). Immediately after attaining

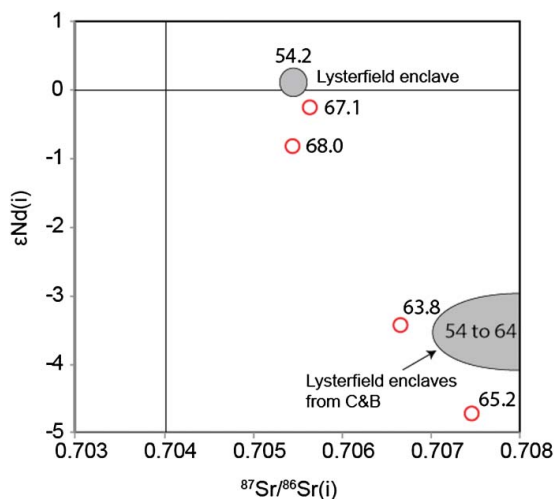


**Figure 15.**  $\epsilon_{\text{Nd}(i)}$  vs  $^{87}\text{Sr}/^{86}\text{Sr}$  plot for granitoids from the Lysterfield pluton. The numbers above each data point indicate the silica content of the rock (in wt%). Although there is a clear trend of  $^{87}\text{Sr}/^{86}\text{Sr}$  vs  $\epsilon_{\text{Nd}(i)}$ , there is no clear trend with silica content, with some of the most silica-rich rocks being the most isotopically primitive. Note how the mafic enclaves cover a similar  $\epsilon_{\text{Nd}(i)}$  range to those of the host granitoids for similar silica contents. Data presented in Table 2 and unpublished data from Maas and Nicholls. The grey field on the lower right shows data from Supplementary Papers Table 3 and Clemens and Bezuidenhout (2014, figure 10).

thermal equilibrium between the hot mafic and the cool silicic magmas, normal discontinuous reactions between crystal and melt may occur and primary pyroxene may react with melt to form aggregates of high-T amphibole and biotite (Vernon, 1990). Accordingly, mafic clots consisting of high-T amphibole (possibly cummingtonite) and biotite (pseudomorphs after pyroxene?) in Tynong Province granitoids are interpreted to result from magma hybridisation.

This field and petrographic evidence is supported by mineral-scale and whole-rock isotopic evidence. In particular, heterogeneous  $\epsilon_{\text{Hf}}$  in magmatic-age zircons records the type of Hf isotopic variation that was attributed to syn-intrusive magma mixing in detailed U–Pb–Hf–O isotopic studies of other I-type granitoids of the Lachlan Fold Belt (Kemp et al., 2007). Whole-rock Sr–Nd isotopic data (Figure 15) are consistent with a magma mixing model, although they also permit other explanations. Correlations between Nd isotopes and major-element compositions in the large Tynong granodiorite, its enclaves and hybrid zones, are tentatively interpreted here as support for intrusion-wide magma mixing activity.

## Conclusions

In combination, the field, petrographic and chemical–isotopic evidence presented here suggests that syn-granite magma hybridisation (by mingling and mixing), together with fractionation and assimilation, were important processes in the formation of the Tynong Province granites, rather than a localised event of minor importance (Clemens & Bezuidenhout, 2014; Clemens et al., 2016). The microgranitoid enclaves, which are mostly more mafic than the granitoids, and common in most outcrops of the Tynong Province, are accepted

here as remnants of incompletely hybridised mafic magmas, as snapshots of the complex mixing process. Their isotopic and chemical compositions are not always easily fitted with simple two-component mixing models. Similar inconsistencies are common in enclave suites elsewhere and have triggered much of the debate about their origin and significance and about the importance of magma mixing in general. Initial Sr isotope compositions in Tynong Province enclaves substantially overlap those of their felsic host rocks, and a partial overlap is observed for Nd isotopes. The coupled changes in Sr–Nd and major-element compositions expected in simple mixing models are not widely observed, although our data for the Tynong granodiorite may be a rare exception. Decoupling of chemical and isotopic signatures is attributed to a history of multiple magma hybridisation events interspersed with periods of magma fractionation and/or assimilation, producing multiple and probably transient magma components and mixing trends. Involvement of substantial mafic–intermediate magmas in Tynong Province magmatism implies the presence of voluminous mafic magmas in the lower crust, both as a source of heat for the ca 370 Ma thermal event in the Melbourne Zone and beyond, and as a component in the granitoids. Mafic magmatism preserved in the form of andesites interbedded with 370 Ma rhyodacitic ignimbrite sheets in the Cerberean Cauldron caldera complex (VandenBerg et al., 2000), extensive mafic dykes in the Woods Point Dyke Swarm (e.g. Bierlein et al., 2001) and the—possibly slightly older—Mt Buller/Mt Stirling gabbro–diorite–tonalite complex (Soesoo, 2000) are examples of such mantle-derived magmatism in the region at this time.

## Acknowledgements

We thank Ron Vernon, Tracy Rushmer and an anonymous reviewer for their comments that helped us improve this manuscript. This research was funded by the ARC Discovery Project DP110102543.

## Disclosure statement

No potential conflict of interest was reported by the authors.

## References

- Acosta-Vigil, A., London, D., & Morgan, G. B. (2012). Chemical diffusion of major components in granitic liquids: Implications for the rates of homogenization of crustal melts. *Lithos*, 153, 308–323.
- Adams, C. J., Pankhurst, R. J., Maas, R., & Millar, I. L. (2005). Nd and Sr isotopic signatures of metasedimentary rocks around the South Pacific margin and implications for their provenance. In A. P. M. Vaughan, P. T. Leat & R. J. Pankhurst (Eds.), *Terrane processes at the margins of Gondwana* (Vol. 246, pp. 113–141). London, UK: Geological Society of London, Special Publication.
- Barbarin, B., & Didier, J. (1992). Genesis and evolution of mafic microgranular enclaves through various types of interaction between coexisting felsic and mafic magmas. *Transactions of Royal Society of Edinburgh, Earth Science*, 88, 145–153.
- Baxter, S., & Feely, M. (2002). Magma mixing and mingling textures in granitoids: Examples from the Galway Granite, Connemara, Ireland. *Mineralogy and Petrology*, 76, 63–74.

- Belousova, E. A., Griffin, W. L., & O'Reilly, S. Y. (2006). Zircon crystal morphology, trace element signatures and Hf isotope composition as a tool for petrogenetic modelling: Examples from eastern Australian granitoids. *Journal of Petrology*, 47, 329–353.
- Bierlein, F. P., Arne, D. C., Keay, S. M., & McNaughton, N. J. (2001). Timing relationships between felsic magmatism and mineralisation in the central Victorian gold province, Southeast Australia. *Australian Journal of Earth Sciences*, 48, 883–899.
- Black, L. P., Everard, J. L., McClenaghan, M. P., Korsch, R. J., Calver, C. R., Fioretti, A. M., ... Foudoulis, C. (2010). Controls on Devonian–Carboniferous magmatism in Tasmania, based on inherited zircon age patterns, Sr, Nd and Pb isotopes, and major and trace element geochemistry. *Australian Journal of Earth Sciences*, 57, 933–968.
- Blichert-Toft, J. & Albarède, F. (1997). The Lu–Hf isotope geochemistry of chondrites and the evolution of the mantle–crust system. *Earth Planetary Science Letters*, 148, 243–258. Erratum: *Earth Planetary Science Letters*, 154 (1998), 349.
- Bonin, B. (2004). Do coeval mafic and felsic magmas in post-collisional to within-plate regimes necessarily imply two contrasting, mantle and crust, sources? A review. *Lithos*, 78, 1–24.
- Carlson, R. W., Lugmair, G. W., & Macdougall, J. D. (1981). Columbia River volcanism: The question of mantle heterogeneity or crustal contamination. *Geochimica et Cosmochimica Acta*, 45, 2483–2499.
- Cayley, R. A., Korsch, R. J., Moore, D. H., Costelloe, R. D., Nakamura, A., Willman, C. E., Rawling, T. J., Morand, V. J., Sklandzien, P. B., & O'Shea, P. J. (2011). Crustal architecture of central Victoria: Results from the 2006 deep crustal reflection seismic survey. *Australian Journal of Earth Sciences*, 58, 113–156.
- Cayley, R. A., Taylor, D. H., VandenBerg, A. H. M., & Moore, D. H. (2002). Proterozoic–Early Palaeozoic rocks and the Tynnan Orogeny in central Victoria: The Selwyn Block and its tectonic implications. *Australian Journal of Earth Sciences*, 49, 225–254.
- Chappell, B. W. (1996). Magma mixing and the production of compositional variation within granite suites: Evidence from the granites of southeastern Australia. *Journal of Petrology*, 37, 449–470.
- Chappell, B. W., & White, A. J. R. (1992). I- and S-type granites in the Lachlan Fold Belt. *Transactions Royal Society of Edinburgh: Earth Sciences*, 83, 1–26.
- Chappell, B. W., White, A. J. R., & Wyborn, D. (1987). The importance of residual source material (restite) in granite petrogenesis. *Journal of Petrology*, 28, 1111–1138.
- Chappell, B. W., & Wyborn, D. (2012). Origin of enclaves in S-type granites of the Lachlan Fold Belt. *Lithos*, 154, 235–247.
- Chauvel, C., Lewin, E., Carpentier, M., Arndt, N. T., & Marini, J. C. (2008). Role of recycled oceanic basalt and sediment in generating the Hf–Nd mantle array. *Nature Geoscience*, 1, 64–67.
- Clemens, J. D., & Bezuidenhout, A. (2014). Origins of co-existing diverse magmas in a felsic pluton: The Lysterfield Granodiorite, Australia. *Contributions to Mineralogy and Petrology*, 167, 1–23.
- Clemens, J. D., Regmi, K., Nicholls, I. A., Weinberg, R. F., & Maas, R. (2016). The Tynong pluton, its mafic synplutonic sheets and igneous microgranular enclaves: The nature of the mantle connexion in I-type granitic magmas. *Contributions to Mineralogy and Petrology*, 171, 1–17.
- Clemens, J. D., & Stevens, G. (2012). What controls chemical variation in granitic magmas? *Lithos*, 134–135, 317–329.
- Collins, W. J. (1996). Lachlan Fold Belt granitoids: Products of three component mixing. *Transactions of the Royal Society of Edinburgh: Earth Sciences*, 88, 171–181.
- Collins, W. J. (1998). Evaluation of petrogenetic models for Lachlan Fold Belt granitoids: Implications for crustal architecture and tectonic models. *Australian Journal of Earth Sciences*, 45, 483–500.
- Compston, W. (2004). SIMS U–Pb zircon ages for the Upper Devonian Snobs Creek and Cerberean Volcanics from Victoria, with age uncertainty based on  $UO_2/UO$  v.  $UO/U$  precision. *Journal of the Geological Society*, 161, 223–228.
- de Campos, C. P., Perugini, D., Ertel-Ingrisch, W., Dingwell, D. B., & Poli, G. (2011). Enhancement of magma mixing efficiency by chaotic dynamics: An experimental study. *Contributions to Mineralogy and Petrology*, 161, 863–881.
- Dempster, T. J., Jenkin, G. R. T., & Rogers, G. (1994). The origin of rapakivi texture. *Journal of Petrology*, 35, 963–981.
- Eberz, G. W., Nicholls, I. A., Maas, R., McCulloch, M. T., & Whiteford, D. J. (1990). The Nd- and Sr-isotopic composition of microgranitoid enclaves and their host rocks from the Swifts Creek Pluton, southeast Australia. *Chemical Geology*, 85, 119–134.
- Eggs, S. M., Woodhead, J. D., Kinsley, L. P. J., Mortimer, G. E., Sylvester, P., McCulloch, M. T., Hergt, J. M., & Handler, M. R. (1997). A simple method for the precise determination of  $\geq 40$  trace elements in geological samples by ICPMS using enriched isotope internal standardisation. *Chemical Geology*, 134, 311–326.
- Eklund, O., & Shebanov, A. D. (1999). The origin of rapakivi texture by sub-isothermal decompression. *Precambrian Research*, 99, 129–146.
- Elburg, M. A. (1996). Evidence of isotopic equilibrium between microgranitoid enclaves and host granodiorite, Warburton granodiorite, Lachlan Fold Belt, Australia. *Lithos*, 38, 1–22.
- Elburg, M. A., & Nicholls, I. A. (1995). Origin of microgranular enclaves in the S-type Wilson's Promontory Batholith, Victoria: Evidence for magma mingling. *Australian Journal of Earth Sciences*, 42, 423–435.
- Gray, C. M. (1984). An isotopic mixing model for the origin of granitic rocks in southeastern Australia. *Earth and Planetary Science Letters*, 70, 47–60.
- Gray, C. M. (1990). A strontium isotopic traverse across the granitic rocks of southeastern Australia: Petrogenetic and tectonic implications. *Australian Journal of Earth Sciences*, 37, 331–349.
- Gray, C. M., & Kemp, A. I. S. (2009). The two-component model for the genesis of granitic rocks in southeastern Australia—Nature of the metasedimentary-derived and basaltic end members. *Lithos*, 111, 113–124.
- Griffin, W. L., Wang, X., Jackson, S. E., Pearson, N. J., O'Reilly, S. Y., Xu, X., & Zhou, X. (2002). Zircon chemistry and magma mixing, SE China: In-situ analysis of Hf isotopes, Tonglu and Pingtan igneous complexes. *Lithos*, 61, 237–269.
- Hawkesworth, C. J., & Kemp, A. I. S. (2006). Using hafnium and oxygen isotopes in zircons to unravel the record of crustal evolution. *Chemical Geology*, 226, 144–162.
- Hergt, J., Woodhead, J., & Schofield, A. (2007). A-type magmatism in the Western Lachlan Fold Belt? A study of granites and rhyolites from the Grampians region, Western Victoria. *Lithos*, 97, 122–139.
- Hibbard, M. J. (1981). The magma mixing origin of mantled feldspars. *Contribution to Mineralogy and Petrology*, 76, 158–170.
- Hibbard, M. J. (1991). Textural anatomy of twelve magma-mixed granitoid systems. In J. Didier & B. Barbarin (Eds.), *Enclaves and Granite Petrology* (pp. 431–444). Amsterdam: Elsevier.
- Jackson, S. E., Pearson, N. J., Griffin, W. L., & Belousova, E. A. (2004). The application of laser ablation-inductively coupled plasma-mass spectrometry to *in situ* U–Pb zircon geochronology. *Chemical Geology*, 211, 47–69.
- Jacobsen, S. B., & Wasserburg, G. J. (1984). SmNd isotopic evolution of chondrites and achondrites, II. *Earth and Planetary Science Letters*, 67, 137–150.
- Keay, S., Collins, W. J., & McCulloch, M. T. (1997). A three component Sr–Nd isotopic mixing model for granitoid genesis, Lachlan Fold Belt, eastern Australia. *Geology*, 25, 307–310.
- Kemp, A. I. S., & Hawkesworth, C. J. (2003). Granitic perspectives on the generation and secular evolution of the continental crust. In H. D. Holland & K. K. Turekian (Eds.), *Treatise on Geochemistry* (Vol. 3–9, pp. 350–410). Amsterdam: Elsevier.
- Kemp, A. I. S., Hawkesworth, C. J., Foster, G. L., Paterson, B. A., Woodhead, J. D., Hergt, J. M., Gray, C. M., & Whitehouse, M. J. (2007). Magmatic and crustal differentiation history of granitic rocks from Hf–O isotopes in zircon. *Science*, 315, 980–983.
- Kemp, A. I. S., Hawkesworth, C. J., Paterson, B. A., Foster, G. L., Kinny, P. D., Whitehouse, M. J., & Mass, R. (2008). Exploring the plutonic–volcanic link: A zircon U–Pb, Lu–Hf and O isotopic study of paired volcanic and granitic units from southeastern Australia. *Transactions of the Royal Society of Edinburgh: Earth Sciences*, 97, 337–355.

- Kemp, A. I. S., Wormald, R. J., Whitehouse, M. J., & Price, R. C. (2005). Hf isotopes in zircon reveal contrasting sources and crystallisation histories for alkaline to peralkaline granites of Temora, southeastern Australia. *Geology*, 33, 797–800.
- Kretz, R. (1983). Symbols for rock-forming minerals. *American Mineralogist*, 68, 277–279.
- Kurhila, M., Anderson, T., & Ramo, O. T. (2010). Diverse sources of crustal granitic magma: Lu–Hf isotope data on zircon in three Paleoproterozoic leucogranites of southern Finland. *Lithos*, 115, 263–271.
- Ludwig, K. (2000). User's manual for Isoplot 2.4. A geochronological toolkit for Microsoft Excel. Berkeley, California: Berkeley Geochronology Centre. Special Publication.
- Maas, R., Kamenetsky, M. B., Sobolev, A. V., Kamenetsky, V. S., & Sobolev, N. V. (2005). Sr, Nd and Pb isotope evidence for a mantle origin of alkali chlorides and carbonates in the Udachnaya Kimberlite, Siberia. *Geology*, 33, 549–552.
- Maas, R., & Nicholls, I. A. (2012). *Are SE Australia's Paleozoic fold belts underlain by Proterozoic crust? Insights from isotopic studies of Devonian granites*. Paper presented at the 34th International Geological Congress, Brisbane, Australia.
- Maas, R., Nicholls, I. A., & Legg, C. (1997). Igneous and metamorphic enclaves in the S-type Deddick granodiorite, Lachlan fold belt, SE Australia: Petrographic, geochemical and Nd–Sr isotopic evidence for crustal melting and magma mixing. *Journal of Petrology*, 38, 815–841.
- McCulloch, M. T., & Chappell, B. W. (1982). Nd isotopic characteristics of S- and I-type granites. *Earth and Planetary Science Letters*, 58, 51–64.
- McCulloch, M. T., & Woodhead, J. D. (1993). Lead isotopic evidence for deep crustal-scale fluid transport during granite petrogenesis. *Geochimica et Cosmochimica Acta*, 57, 659–674.
- Medlin, C. C., Jowitt, S. M., Cas, R. A. F., Smithies, R. H., Kirkland, C. L., Maas, R. A., ... Wingate, M. T. D. (2014). Petrogenesis of the A-type, mesoproterozoic intra-caldera rheomorphic Kathleen Ignimbrite and Comagmatic Rowland suite intrusions, West Musgrave Province, Central Australia: Products of extreme fractional crystallization in a failed rift setting. *Journal of Petrology*, 56, 493–525.
- Palivcova, M., Waldhausrova, J., & Ledvincova, V. (1995). Ocelli in mafic rocks of granitic complexes. *Krystalinikum*, 22, 149–186.
- Perugini, D., De Campos, C. P., Ertel-Ingrisch, W., & Dingwell, D. B. (2012). The space and time complexity of chaotic mixing of silicate melts: Implications for igneous petrology. *Lithos*, 155, 326–340.
- Perugini, D., & Poli, G. (2012). The mixing of magmas in plutonic and volcanic environments: Analogies and differences. *Lithos*, 153, 261–277.
- Poli, G., Tommasini, S., & Halliday, A. N. (1996). Trace element and isotopic exchange during acid–basic magma interaction processes. *Transactions of the Royal Society of Edinburgh: Earth Sciences*, 87, 225–232.
- Regmi, K. R. (2013). Petrology and geochemistry of the Tynong Province Granitoids, Victoria, Australia. PhD thesis, Monash University, Vic. <http://arrow.monash.edu.au/hdl/1959.1/874311>
- Rossiter, A. G. (2003). Granitic rocks of the Lachlan Fold Belt in Victoria. In W. D. Birch (Ed.), *Geology of Victoria* (Vol. 23, pp. 217–237). Geological Society of Australia Special Publication.
- Rossiter, A. G., & Gray, C. M. (2008). Barium contents of granite: Key to understanding crustal architecture in the southern Lachlan Fold Belt? *Australian Journal of Earth Sciences*, 55, 433–448.
- Sawka, W. N., Heizler, M. T., Kistler, R. W., & Chappell, B. W. (1990). Geochemistry of highly fractionated I- and S-type granites from the tin–tungsten province of western Tasmania. In H. J. Stein & J. L. Hannah (Eds.), *Ore-bearing systems: Petrogenesis and mineralizing processes* (Vol. 246, pp. 161–179). Denver Co: Geological Society of America Special Paper.
- Soesoo, A. (2000). Fractional crystallization of mantle-derived melts as a mechanism from some I-type granite petrogenesis: An example from Lachlan Fold Belt, Australia. *Journal of Geological Society*, 157, 135–149.
- Stacey, J. S., & Kramers, J. D. (1975). Approximation of terrestrial lead isotope evolution by a two-stage model. *Earth and Planetary Science Letters*, 26, 207–221.
- Sun, S. S., & McDonough, W. F. (1989). Chemical and isotopic systematics of oceanic basalts: implications for mantle composition and processes. In A. D. Saunders & M. J. Norry (Eds.), *Magmatism in the ocean basins*. Geological Society of London, London, 42, 313–345.
- Symington, N. J., Weinberg, R. F., Hasalová, P., Wolfram, L. C., Raveggi, M., & Armstrong, R. A. (2014). Multiple intrusions and remelting-remobilization events in a magmatic arc: The St. Peter Suite, South Australia. *Bulletin of the Geological Society of America*, 126, 1200–1218.
- Taylor, S. R., & McLennan, S. M. (1985). *The Continental Crust: Its Composition and Evolution*. Oxford: Blackwell.
- Taylor, S. R., & McLennan, S. M. (1995). The geochemical evolution of the continental crust. *Reviews of Geophysics*, 33, 241–265.
- Tzikas, A. (2002). *Geology and geochemistry of the Mornington Peninsula granites*, BSc (Hons) thesis, Monash University.
- Ubide, T., Galé, C., Larrea, P., Arranz, E., Lago, M., & Tierz, P. (2014). The relevance of crystal transfer to magma mixing: A case study in composite dykes from the central pyrenees. *Journal of Petrology*, 55, 1535–1559.
- Van Achterbergh, E., Ryan, C. G., Jackson, S. E., & Griffin, W. L. (2001). Data reduction software for LA-ICP-MS: Appendix. In P. J. Sylvester (Ed.), *Laser Ablation-ICP-Mass Spectrometry in the Earth Sciences: Principles and Applications* (Vol. 29, pp. 239–243). Ottawa Canada: Mineralogical Association of Canada (MAC) Short Course Series.
- Vance, D., & Thirlwall, M. (2002). An assessment of mass discrimination in MC-ICPMS using Nd isotopes. *Chemical Geology*, 185, 227–240.
- VandenBerg, A. H. M., Willman, C. E., Maher, S., Simons, B. A., Cayley, R. A., Taylor, D. H., Morand, V. J., Moore, D. H., & Radojkovic, A. (2000). The Tasman Fold Belt System in Victoria. Melbourne Vic: Geological Survey of Victoria, Special Publication, 462.
- Vernon, R. H. (1990). Crystallisation and hybridism in microgranitoid enclave magmas: Microstructural evidence. *Journal of Geophysical Research*, 95, 17 849–17 859.
- Vernon, R. H. (2007). Problems in identifying restite in granites of southeastern Australia, with speculations on sources of magma and enclaves. *Canadian Mineralogist*, 45, 147–178.
- Vernon, R. H., Etheridge, M. E., & Wall, V. J. (1988). Shape and microstructure of microgranitoid enclaves: Indicators of magma mingling and flow. *Lithos*, 22, 1–11.
- Vervoort, J. D., Patchett, P. J., Blichert-Toft, J., & Albarède, F. (1999). Relationships between Lu–Hf and Sm–Nd isotopic systems in the global sedimentary system. *Earth and Planetary Science Letters*, 168, 79–99.
- Villaros, A., Buick, I. S., & Stevens, G. (2012). Isotopic variations in S-type granites: An inheritance from a heterogeneous source? *Contributions to Mineralogy and Petrology*, 163, 242–257.
- Waight, T., Baker, J., & Willigers, B. (2002). Rb isotope dilution analyses by MC-ICPMS using Zr to correct for mass fractionation: Towards improved Rb–Sr geochronology? *Chemical Geology*, 186, 99–116.
- Waight, T. E., Dean, A. A., Maas, R., & Nicholls, I. A. (2000). Sr and Nd isotopic investigations towards the origin of feldspar megacryst in microgranular enclaves in two I-type plutons of the Lachlan Fold Belt, southeast Australia. *Australian Journal of Earth Sciences*, 47, 1105–1112.
- Wall, V. J., Clemens, J. D., & Clarke, D. B. (1987). Models for granitoid evolution and source compositions. *Journal of Geology*, 95, 731–749.
- Wark, D. A., & Stimac, J. A. (1992). Origin of mantle (rapakivi) feldspars: Experimental evidence of a dissolution and diffusion-controlled mechanism. *Contributions to Mineralogy and Petrology*, 111, 345–361.
- White, A. J. R., & Chappell, B. W. (1977). Ultrametamorphism and granitoid genesis. *Tectonophysics*, 43, 7–22.
- Wiebe, R. A. (1993). The Pleasant Bay gabbro diorite, coastal Maine: Ponding and crystallization of basaltic injection into a silicic magma chamber. *Journal of Petrology*, 34, 461–489.
- Wiebe, R. A. (1994). Silicic magma chambers as traps for basaltic magmas: The Cadillac intrusive complex, Mount Desert Island, Maine. *Journal of Geology*, 102, 423–437.
- Wiedenbeck, M., Alle, P., Corfu, F., Griffin, W. L., Meier, M., Oberli, F., ... Spiegel, W. (1995). Three natural zircon standards for U–Th–Pb, Lu–Hf, trace element and rare earth elements analyses. *Geostandards Newsletter*, 19, 1–23.
- Willman, C. E., Korsch, R. J., Moore, D. H., Cayley, R. A., Lisitsin, V. A., Rawling, T. J., Morand, V. J., & O'Shea, P. J. (2010). Crustal-scale fluid pathways and source rocks in the Victorian gold province, Australia:

- Insights from deep seismic reflection profiles. *Economic Geology*, 105, 895–915.
- Woodhead, J. D., & Hergt, J. M. (2005). A preliminary appraisal of seven natural zircon reference materials for *in situ* Hf isotope determination. *Geostandards and Geoanalytical Research*, 29, 183–195.
- Woodhead, J. D., Hergt, J. M., Shelley, M., Eggin, S., & Kemp, R. (2004). Zircon Hf-isotope analysis with an excimer laser, depth profiling, ablation of complex geometries, and concomitant age estimation. *Chemical Geology*, 209, 121–135.
- Wyborn, D., Chappell, B. W., & James, M. (2001). Examples of convective fractionation in high-temperature granites from the Lachlan Fold Belt. *Australian Journal of Earth Sciences*, 48, 531–542.
- Wyllie, P. J., Cox, K. G., & Biggar, G. M. (1962). The habit of apatite in synthetic systems and igneous rocks. *Journal of Petrology*, 3, 238–243.
- Yang, J.-H., Wu, F.-Y., Wilde, S. A., Xie, L.-W., Yang, Y.-H., & Liu, X.-M. (2007). Tracing magma mixing in granite genesis: *In situ* U–Pb dating and Hf-isotope analysis of zircons. *Contributions to Mineralogy and Petrology*, 153, 177–190.
- Zheng, Y. F., Zhang, S. B., Zhao, Z. F., Wu, Y. B., Li, X., Li, Z., & Wu, F. Y. (2007). Contrasting zircon Hf and O isotopes in the two episodes of Neoproterozoic granitoids in South China: Implications for growth and reworking of continental crust. *Lithos*, 96, 127–150.